

Systematic experimental charge density analysis of anion receptor complexes

Isabelle L. Kirby,^a Mark Brightwell,^a Mateusz B. Pitak,^a Claire Wilson,^b Simon J. Coles^{*,a} and Philip A. Gale^{*,a}

^a Chemistry, University of Southampton, Southampton, UK, SO17 1BJ. E-mail: s.j.coles@soton.ac.uk; philip.gale@soton.ac.uk

^bDiamond Light Source, Diamond House, Harwell Science and Innovation Campus, Didcot, Oxfordshire, UK, OX11 0DF

Supporting Information

Contents:

1)	Experimental	3
a.	Synthesis	3
b.	Crystallisation	4
c.	X-ray diffraction data collection details	4
d.	Table of crystallographic data	6
2)	Electron density maps	7
a.	Residual density maps of structures 4 – 8	7
b.	Fractal dimension distribution of residual density plots	9
c.	Static deformation density maps of structures 4 – 8	12
d.	Negative $-\nabla^2\rho(r)$ maps of structures 4 – 8	15
e.	Bond path plots of structures 4 – 8	17
3)	Topological Properties	21
a.	Electronic properties of covalent bond BCPs in structures 4 – 8	21
b.	Bond ellipticity profiles of the aromatic bonds	26
c.	Bond ellipticity and Laplacian profiles of the bonds of the urea moiety	
		30
4)	QTAIM Charges of atoms in structures 4 - 8	39
a.	QTAIM charges of 4	39
b.	QTAIM charges of 5	40
c.	QTAIM charges of 6	41
d.	QTAIM charges of 7	42
e.	QTAIM charges of 8	44

5)	Proton NMR Titration Studies	46
a.	Methodology	46
b.	Stack Plot and Fit Plot for receptor 1 with TMA acetate	46
c.	Stack Plot and Fit Plot for receptor 1 with TBA chloride	47
d.	Stack Plot for receptor 1 with TBA fluoride	48
e.	Stack Plot for receptor 1 with TBA hydroxide	49
f.	Stack Plot of receptor 2 with TBA chloride	49
g.	Stack Plot and Fit Plot of receptor 3 with TMA acetate	50
h.	Stack Plot for receptor 3 with TBA hydroxide	51
6)	References	52

1) Experimental

a. Synthesis

1,3-Bis(4-nitrophenyl)urea, **1**, was synthesised according to literature procedures.¹ 4-Nitrophenylisocyanate (0.38 g, 2.40×10^{-3} moles, 1.6 eq) was dissolved in dichloromethane (50 mL). 4-Nitroaniline (0.20 g, 1.50×10^{-3} moles, 1.0 eq) was added followed by triethylamine (0.50 mL, 1.60×10^{-3} moles, 1.0 eq) and the solution stirred overnight. The resulting solid was isolated by filtration and washed with dichloromethane, and the solid was recrystallised from acetonitrile. This resulted in a yellow powder (0.078 g, 2.50×10^{-4} moles, 17 %). MP > 300 °C (literature value 310 °C)¹ ¹H NMR (300 MHz, d₆-DMSO) 7.73 ppm (d, 9.4 Hz, 4H, CH), 8.22 ppm (d, 9.0 Hz, 4H, CH), 9.66 ppm (br. s., 2H, NH) (consistent with literature reference)²

1,3-Bis(3-nitrophenyl)urea, **2**, was synthesised according to literature procedures.¹ 3-Nitrophenylisocyanate (0.36 g, 2.40×10^{-3} mol, 1.5 eq) was dissolved in dichloromethane (50 mL). 3-Nitroaniline (0.20 g, 1.50×10^{-3} mol, 1.0 eq) was added followed by triethylamine (0.50 mL, 1.60×10^{-3} mol, 1.0 eq) and the solution stirred overnight. The resulting solid was isolated by filtration and washed with dichloromethane, and the solid was recrystallised from chloroform and hexane. This resulted in a yellow solid (0.37 g, 1.20×10^{-3} moles, 80 %). MP = 250-252°C (literature value 256-258°C)³ ¹H NMR (300 MHz, d₆-DMSO) 7.59 ppm (t, 8.3 Hz, 2H, CH), 7.77 ppm (d, 6.8 Hz, 2H, CH), 7.85 ppm (d, 6.8 Hz, 2H, CH), 8.55 ppm (t, 2.0 Hz, 2H, CH), 9.75 ppm (br. s., 2H, NH) (consistent with literature reference)³

1,3-Bis(3,5-di-nitrophenyl)urea, **3**, was synthesised according to literature procedures.⁴ 3,5-Dinitrophenylisocyanate (0.12 g, 5.50×10^{-4} mol, 1.0 eq) was dissolved in toluene (50 mL). 3,5-Dinitroaniline (0.10 g, 5.50×10^{-4} mol, 1.0 eq) was added followed by triethylamine (2.00 mL, 1.43×10^{-2} mol, 26.0 eq). The reaction was heated at reflux overnight under a nitrogen atmosphere. A precipitate formed and this was isolated by filtration to yield a pale yellow solid (0.098 g, 2.50×10^{-4} mol, 45%). MP: >270°C (decomposition) (consistent with literature value of 306°C in acetone)⁵. ¹H NMR (300 MHz, d₆-DMSO): 8.46 ppm (t, 1.8 Hz, 2H, CH), 8.80 ppm

(d, 1.8 Hz, 4H, CH), 10.13 ppm (s, 2H, NH) ^{13}C NMR: (75 MHz, d₆-DMSO): 111.5 ppm (CH, +DEPT), 118.4 ppm (CH, +DEPT), 141.5 ppm (q, Ar C), 148.2 ppm (q, Ar C), 152.3 ppm (q, C=O) LR ESI $^-$: m/z: 391.0 [M-H] $^-$ (100%), 392.2 [M-H] $^-$ (^{13}C isotope 12%)

b. Crystallisation

Crystals of **4** and **5** were grown by vapour diffusion of diethyl ether into a solution of the corresponding tetramethylammonium salt and receptor **1** in acetonitrile.

Crystals of **6** were grown by slow evaporation of an acetonitrile solution of tetramethylammonium fluoride and **1**.

Crystals of **7** were grown by vapour diffusion of diethyl ether into an isopropanol solution of tetramethylammonium chloride and receptor **2**.

Crystals of **8** were obtained by vapour diffusion of diethyl ether into a mixed acetonitrile and methanol solution of tetramethylammonium acetate and receptor **3**.

c. High-resolution X-ray Diffraction Experiments

Two of the data sets used in this study (**4** and **5**) were collected on our home source diffractometers. The remaining three data sets (**6**, **7** and **8**) were collected on the small molecule single crystal diffraction beamline I19 at Diamond Light source⁶.

Beamline

Beamline I19 is situated on an in-vacuum undulator insertion device. The wavelength is selected using a cryo-cooled double-crystal monochromator with a Si-111 crystal set. Beam focussing can be carried out using a pair of bimorph mirrors that independently focus the beam in the vertical and horizontal axes. For the data collections reported herein two configurations of the beamline were used. For **6** and **8** data were collected at a wavelength of 0.6889 Å and using the bimorph mirrors set to provide a slightly defocused beam at the sample positions. Data for **7** were collected at 0.4859 Å and without the mirror focussing.

Data collection and reduction

Diffraction data were collected in Experimental Hutch 1 (EH1), which is equipped with a Crystal Logic 4-circle kappa geometry diffractometer and a Rigaku Saturn 724+ CCD detector. The samples were cooled to and maintained at 100 K using an Oxford Cryosystems Cryostream plus. Diffractometer control and data processing were carried out using CrystalClear-SM Expert 2.0⁷.

Data were collected according to a calculated strategy to satisfy the criteria of 100% completeness with a 10-fold redundancy to a given resolution limit of 0.45 Å for **6** and **8** and 0.35 Å in the case of **7**, where with the shorter wavelength higher resolution data were accessible. Two detector swing angle settings were used for these calculated strategies – 30° and 70° for **6** and **8** and 30 and 60 degrees for **7**. Additional data were collected with a detector swing angle of 0° for **7** and **8** to ensure that a complete set of low angle reflections were collected and none were lost through peak saturation. This was planned for **6** as well but unfortunately the crystal was lost part way through the data collection and not all planned data were collected. A second dataset for this system was collected on a different and considerably smaller crystal however, due to its higher quality, the first, less complete than intended data set was used. Different exposure times (ranging between 0.5 second to 6 second exposure per degree), image widths (0.5 and 1°) and levels of attenuation were used for each of the detector settings and for each of the samples. The total data collection times were approximately 3 hours (cut short through crystal loss), 7 hours and 9 hours for **6**, **7** and **8** respectively.

In each case data for the individual detector swing angle settings were integrated separately⁷ and then the 3 subsets scaled and merged together using SORTAV⁸. Further experimental details are given in Table S1.

Laboratory source data

A similar approach was used to collect the diffraction data for both **4** and **5** which were collected using laboratory sources: a Bruker-Nonius KappaCCD area detector diffractometer on a Bruker-Nonius FR591 rotating anode generator and a Rigaku AFC 12 diffractometer mounted on Rigaku FR-E+ Super Bright Very High Flux rotating anode CCD diffractometer equipped with VariMax very high flux (VHF) optics and Saturn 724+ CCD detector, respectively.

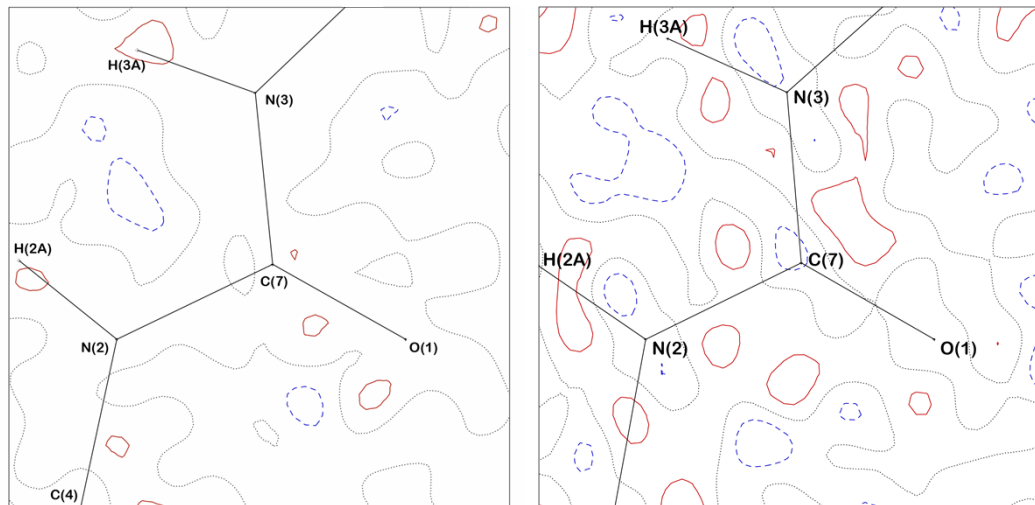
Experimental details are given in Table S1.

d. Table S1: Crystallographic data for structures **4 - 8**.

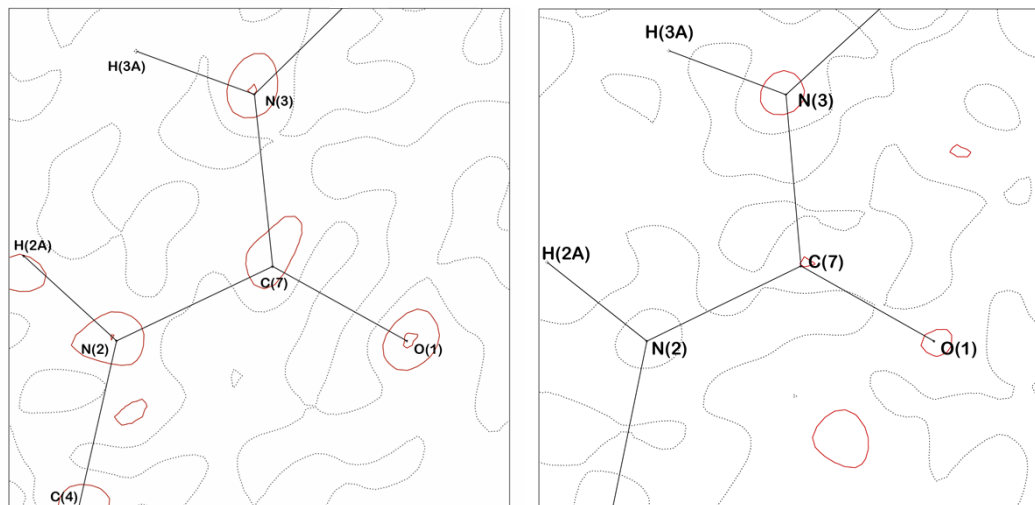
Compound	4	5	6	7	8
Chemical formula	C ₁₇ H ₂₂ ClN ₅ O ₅	C ₁₉ H ₂₅ N ₅ O ₇	C ₃₀ H ₃₂ FN ₉ O ₁₀	C ₁₇ H ₂₂ ClN ₅ O ₅	C ₁₉ H ₂₃ N ₇ O ₁₁
Formula weight	411.85	435.44	697.65gmol ⁻¹	411.85	525.44
Crystal system and space group	Triclinic <i>P</i> -1	Triclinic <i>P</i> -1	Orthorhombic <i>P</i> ca	Orthorhombic <i>Pna</i> 2 ₁	Triclinic <i>P</i> -1
a (Å)	7.6033 (2)	7.797 (2)	35.929 (6)	6.8211 (5)	9.602 (3)
b (Å)	11.4827 (3)	11.214 (3)	7.0153 (11)	14.4139 (11)	10.807 (3)
c (Å)	11.8705 (4)	12.211 (3)	12.624 (2)	19.7918 (16)	12.433 (4)
α (°)	83.1860 (10)	91.753 (5)	90	90	109.859 (5)
β (°)	71.662 (2)	104.560 (7)	90	90	96.598 (3)
γ (°)	80.423 (2)	95.232 (13)	90	90	103.5372 (5)
V (Å ³)	967.59 (5)	1027.5 (5)	3181.9 (9)	1945.9 (3)	1152.7 (6)
Z	2	2	4	4	2
λ (Å)	0.71073	0.71073	0.68890	0.48590	0.68890
μ (mm ⁻¹)	0.237	0.109	0.106	0.093	0.116
F(000)	432.0	460.0	1456.0	863.8	548.0
Crystal morphology	Yellow block	Yellow column	Yellow prism	Yellow block	Yellow plate
Crystal size (mm)	0.60 x 0.24 x 0.20	0.40 x 0.08 x 0.08	0.10 x 0.07 x 0.04	0.18 x 0.05 x 0.05	0.12 x 0.10 x 0.08
(sin θ / λ) _{max} (Å ⁻¹)	1.1582	1.2372	1.1101	1.4597	1.1124
(sin θ / λ) _{trunc} (Å ⁻¹)	1.10	1.10	1.00	1.40	1.06
No. of collected/unique reflections	356257/ 25085	147512/ 46630	159791/ 18948	363541/ 51978	179628/ 23530
R _{merge}	0.0457	0.0812	0.0308	0.0663	0.0742
Overall completeness to (sin θ / λ) _{max} (%)	99.6	95.9	95.7	99.5	88.6
Index ranges	-16 ≤ h ≤ 17 , -26 ≤ k ≤ 26 0 ≤ l ≤ 27	-19 ≤ h ≤ 18 , -27 ≤ k ≤ 27 0 ≤ l ≤ 30	0 ≤ h ≤ 76 , 0 ≤ k ≤ 15 0 ≤ l ≤ 27	-19 ≤ h ≤ 19 , 0 ≤ k ≤ 41 0 ≤ l ≤ 57	-21 ≤ h ≤ 21 , -24 ≤ k ≤ 22 0 ≤ l ≤ 25
Overall redundancy	14.3	4.7	8.4	7	7.6
Absorption correction type	multi-scan	multi-scan	multi-scan	multi-scan	multi-scan
T _{min} /T _{max}	0.8708/ 0.9541	0.9577/ 0.9913	0.9886/ 0.9954	0.9770/ 0.9935	0.9850/ 0.9900
<i>spherical refinement</i>					
R indices (all data)	R1 = 0.077, wR2 = 0.121	R1 = 0.087, wR2 = 0.167	R1 = 0.048, wR2 = 0.141	R1 = 0.053, wR2 = 0.095	R1 = 0.067, wR2 = 0.146
Final R indices [F ² > 2σ(F ²)]	R1= 0.048, wR2 = 0.104	R1 = 0.072, wR2 = 0.152	R1 = 0.044, wR2 = 0.136	R1 = 0.037, wR2 = 0.083	R1 = 0.056, wR2 = 0.134
Δρ(r) (e Å ⁻³)	-0.352/0.636	-0.599/0.721	-0.439/0.568	-0.342/0.861	-0.490/1.153
<i>multipole refinement</i>					
R(F)	0.0377	0.0531	0.0293	0.0381	0.0396
R(F ²)	0.0279	0.0519	0.0362	0.0329	0.0520
Goodness of fit	1.3971	1.6452	2.0665	1.1727	1.6196
Max sin(θ/λ) used in refinement	1.10	1.10	1.00	1.40	1.06
Data/parameter ratio	23.25	25.99	21.29	48.90	18.95
Δρ(r) (e Å ⁻³)	-0.334/0.619	-0.304/0.354	-0.396/0.392	-0.329/0.540	-0.432/0.451

2) Electron density maps

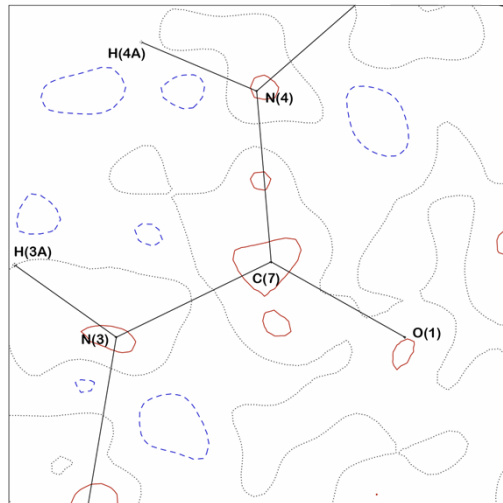
a. Residual density maps



Residual electron density maps: Left: 4 Right: 5



Residual electron density maps: Left: 6 Right: 7



Residual electron density map: 8

Figure S1: Residual electron density plots after multipole refinement in the plane of the urea group of the receptor molecule. Positive electron density is shown in red and negative electron density in blue. Zero-level contours are dashed. Contours are at $0.1 \text{ e } \text{\AA}^{-3}$ with cut-off at $0.9 \text{ e } \text{\AA}^{-3}$.

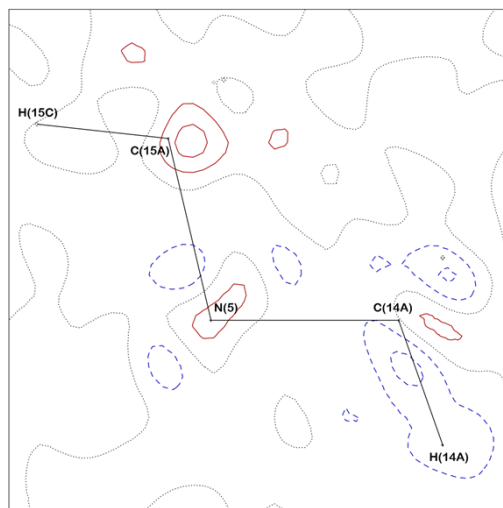


Figure S2: Residual density plots after multipole refinement (with multipole parameters for the tetramethylammonium (TMA) cation taken from the INVARIOM database⁹) in the plane of the TMA cation. Positive electron density is shown in red and negative electron density in blue. Zero-level contours are dashed. Contours are at $0.1 \text{ e } \text{\AA}^{-3}$ with cut-off at $0.9 \text{ e } \text{\AA}^{-3}$.

b. Fractal dimension distribution of residual density plots¹⁰

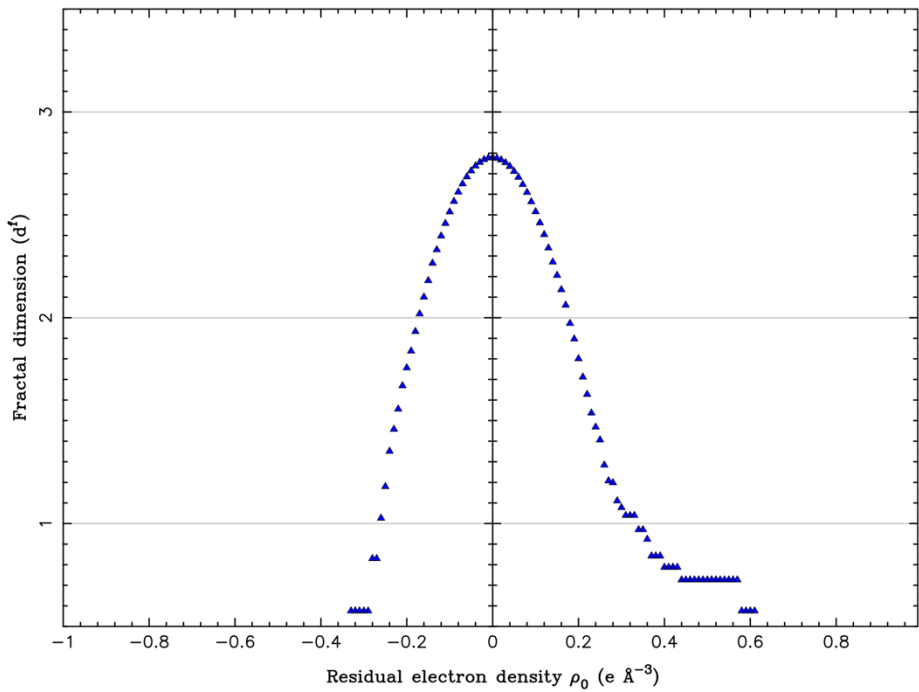


Figure S3: Fractal dimension distribution of residual density plot of 4

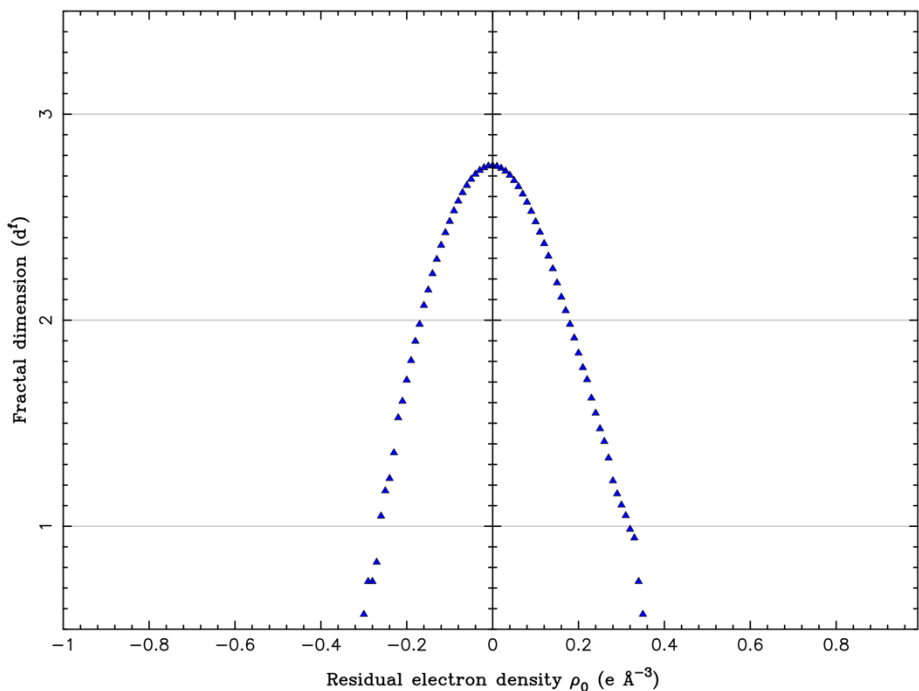


Figure S4: Fractal dimension distribution of residual density plot of 5

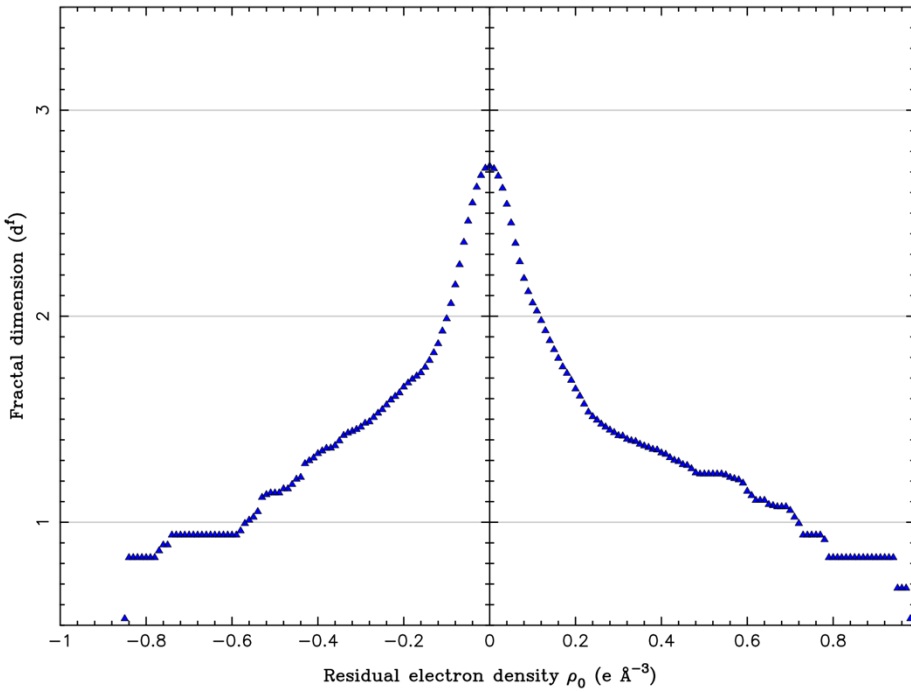


Figure S5: Fractal dimension distribution of residual density plot of **6** modelled ignoring disorder of TMA group. The large residual electron density seen is located around the TMA cation. The methyl carbons of this group have large thermal displacement parameters. Attempts to obtain a very low temperature dataset (30 K) were hampered by a phase transition and so the 100 K dataset was used and the TMA CH_3 groups constrained with $3m$ symmetry, however this did not reduce the residual el. density.

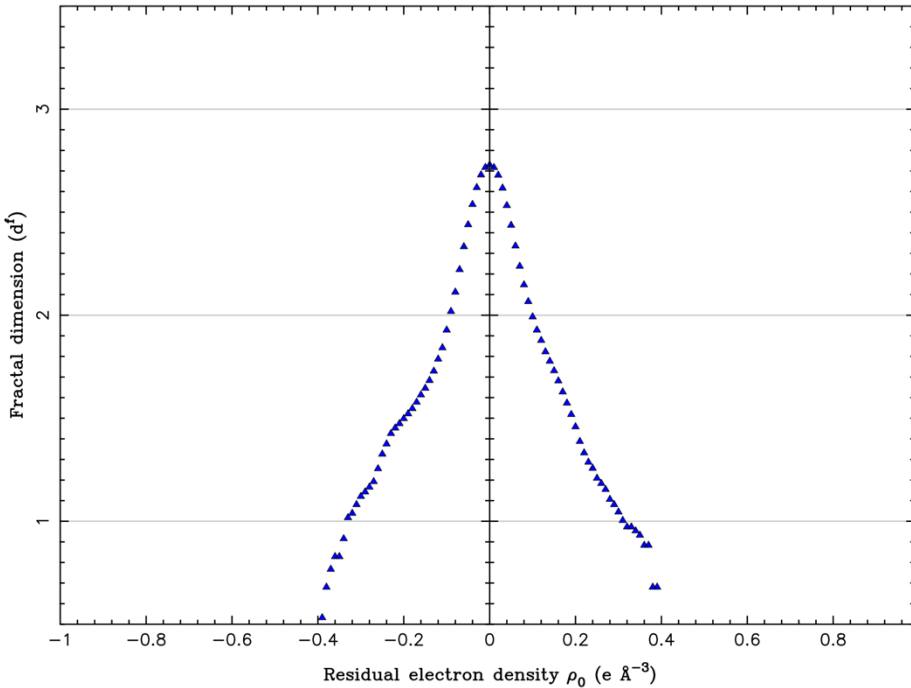


Figure S6: Fractal dimension distribution of residual density plot of **6** after disorder refinement of TMA cation and INVARIOM multipole population transfer for TMA group, and refinement of the final model. The plot shows that the residual density has been markedly reduced following this strategy and that it is now distributed in a Gaussian-like manner, suggesting that it is noise and all the density has been incorporated into the model. This illustrates the improvement in the final model.

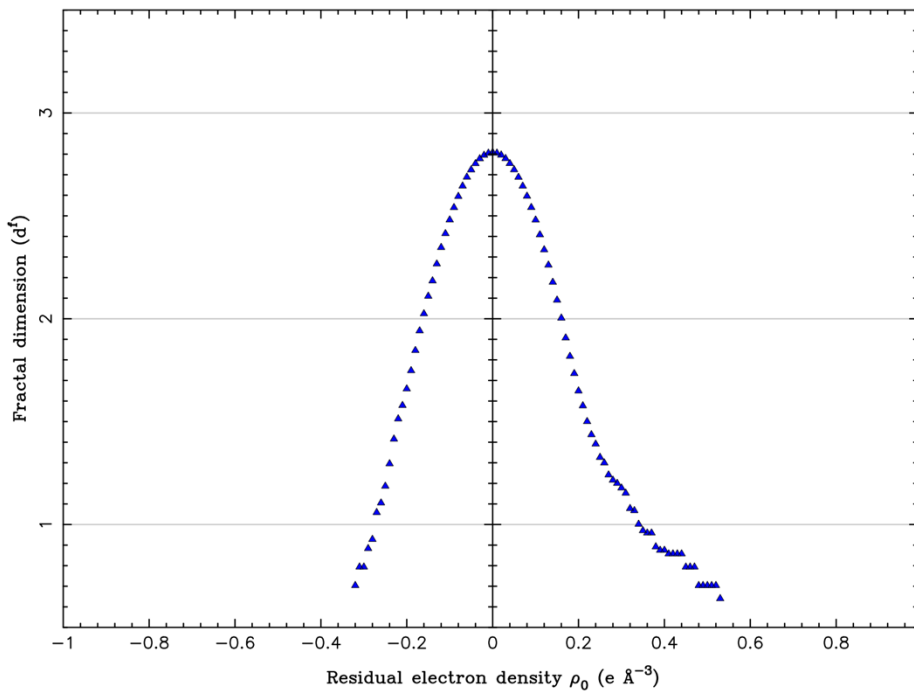


Figure S7: Fractal dimension distribution of residual density plot of 7

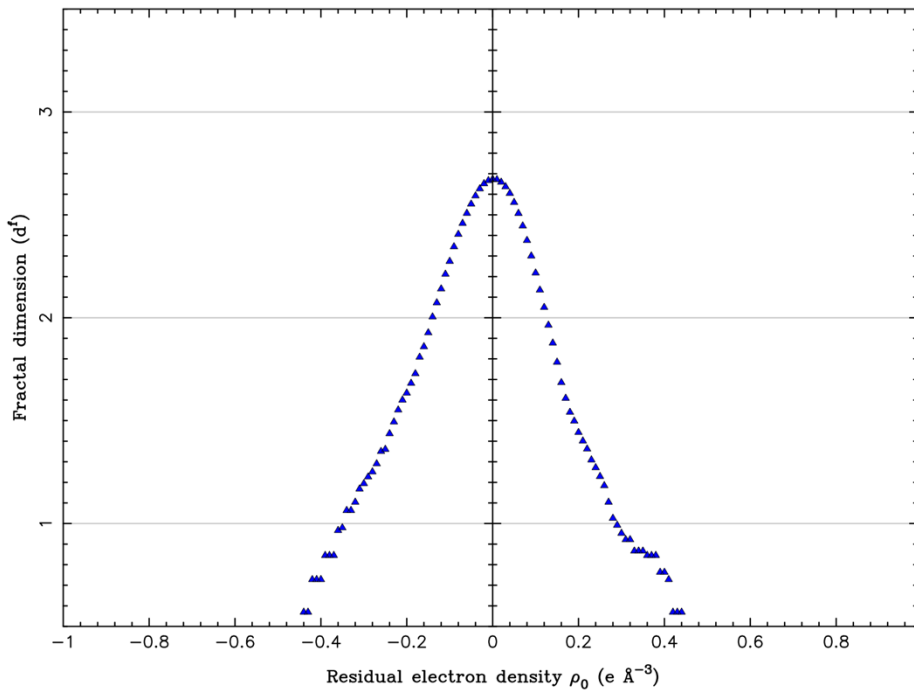


Figure S8: Fractal dimension distribution of residual density plot of 8

c. Static deformation charge density distribution maps

Static deformation charge density distribution maps plotted in the plane of urea group of the receptor molecule after multipole refinement. Positive electron density shown in red, negative electron density in blue. Zero contours are dashed. Contours are at 0.1 $e \text{ \AA}^{-3}$.

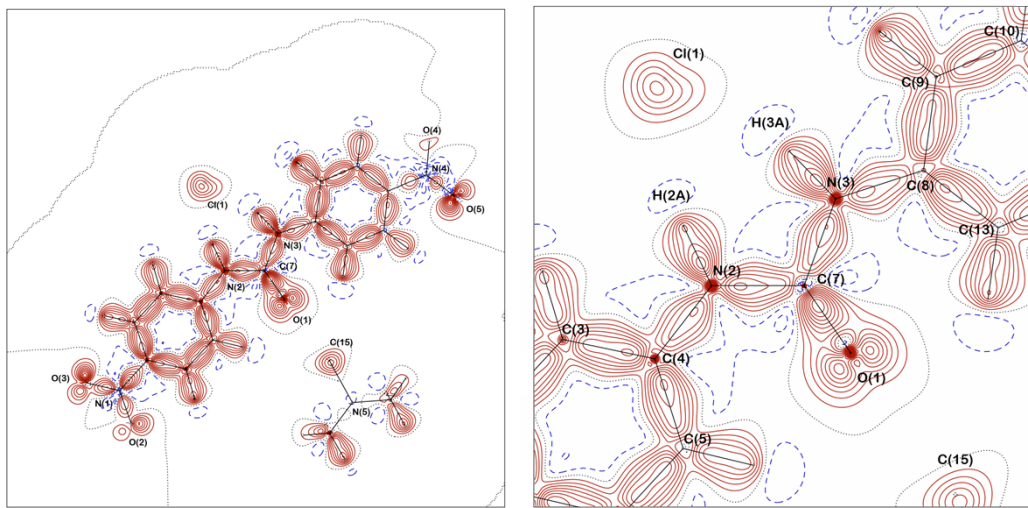


Figure S9: Static deformation charge density distribution maps of whole receptor molecule (left) and anion binding region (right) of structure 4. The chloride anion, nitro groups and TMA groups displayed do not lie in the plane of the urea in which the map was drawn.

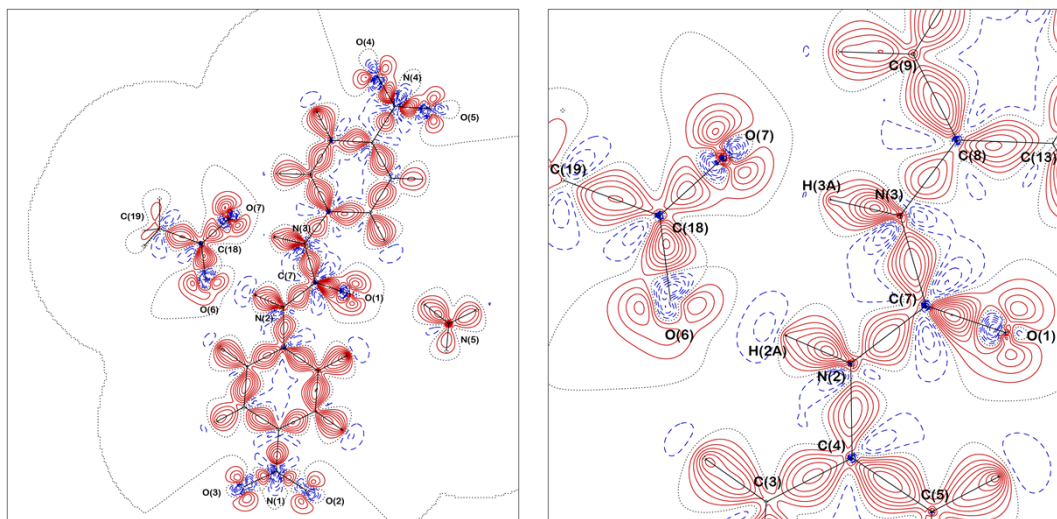


Figure S10: Static deformation charge density distribution maps of whole receptor molecule (left) and anion binding region (right) of structure 5. The TMA group and nitro groups displayed do not lie in the plane of the urea in which the map was drawn.

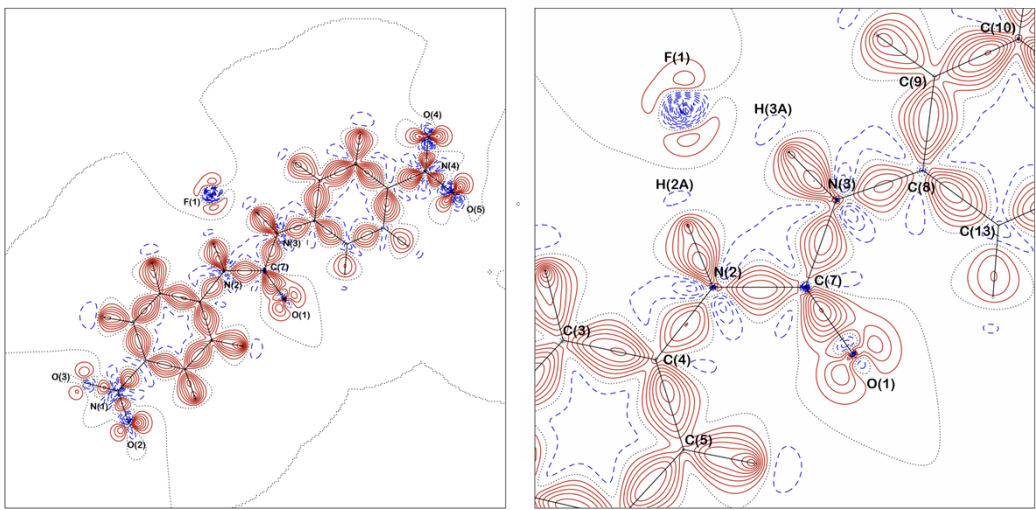


Figure S11: Static deformation charge density distribution maps of whole receptor molecule (left) and anion binding region (right) of structure **6**. The nitro groups and TMA group displayed do not lie in the plane of the urea in which the map was drawn.

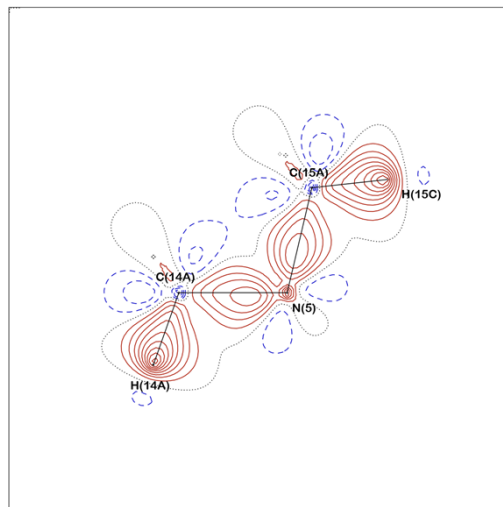


Figure S12: Static deformation charge density distribution map of part of the TMA group of **6** after INVARIOM based multipole refinement of the crystal structure.

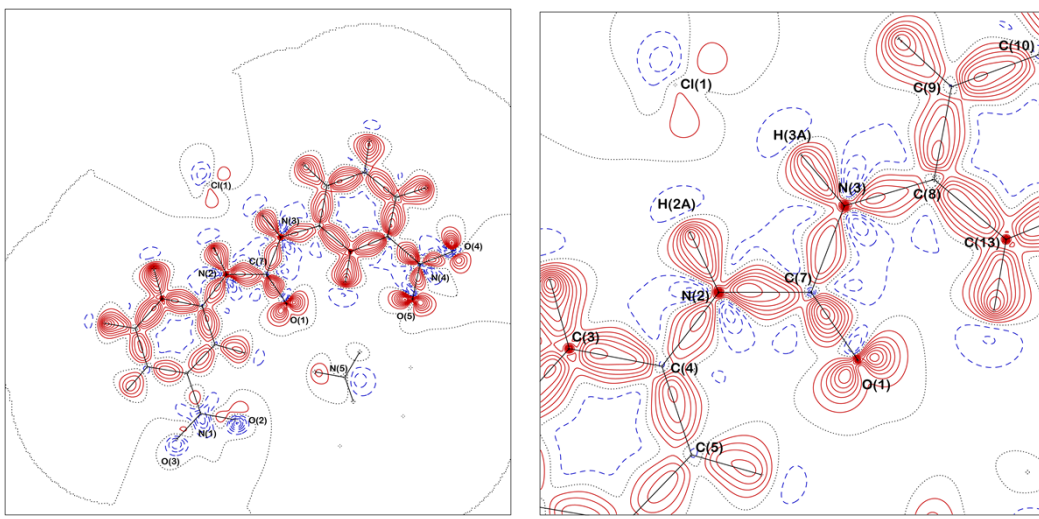


Figure S13: Static deformation charge density distribution maps of whole receptor molecule (left) and anion binding region (right) of structure 7. The chloride anion, nitro groups and TMA groups displayed do not lie in the plane of the urea in which the map was drawn.

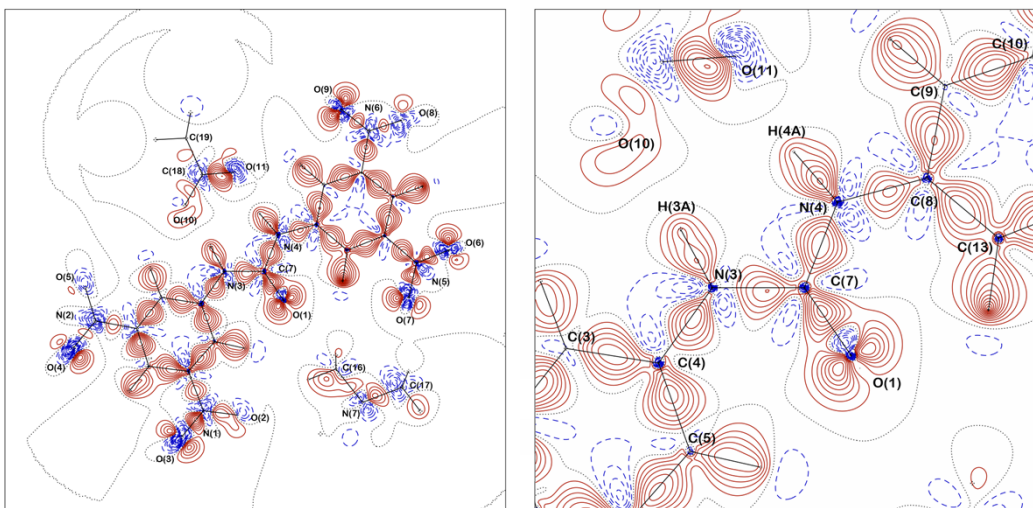


Figure S14: Static deformation charge density distribution maps of whole receptor molecule (left) and anion binding region (right) of structure **8**. The acetate anion, nitro groups and TMA groups displayed do not lie in the plane of the urea in which the map was drawn.

d. $-\nabla^2\rho(r)$ maps

$-\nabla^2\rho(r)$ charge density distribution maps in the plane of urea group of the receptor molecule after multipole refinement. Positive electron density shown in red, negative electron density in blue. Contours are in a logarithmic scale, $e \text{ \AA}^{-5}$.

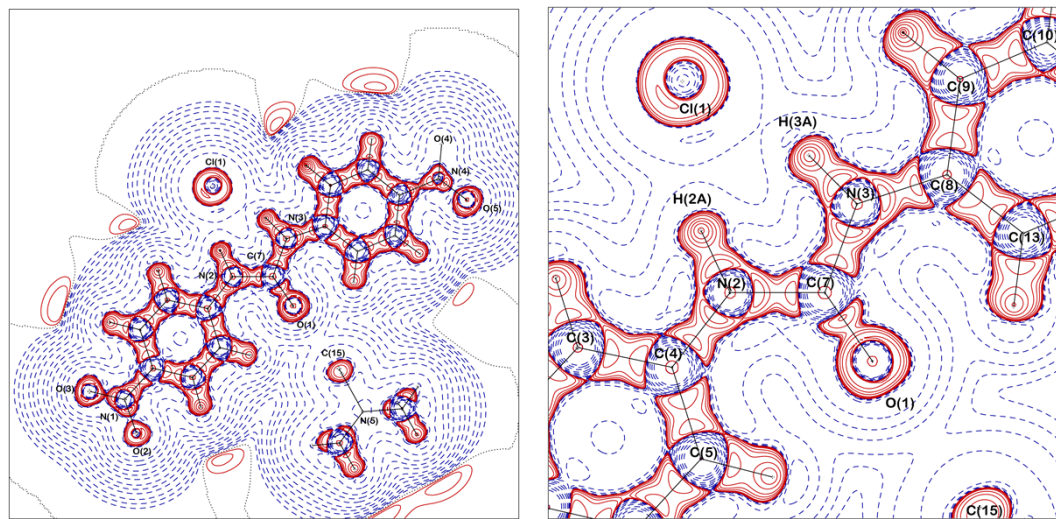


Figure S15: $-\nabla^2\rho(r)$ charge density distribution maps of whole receptor molecule (left) and anion binding region (right) of structure 4. Map drawn in the plane of the urea group.

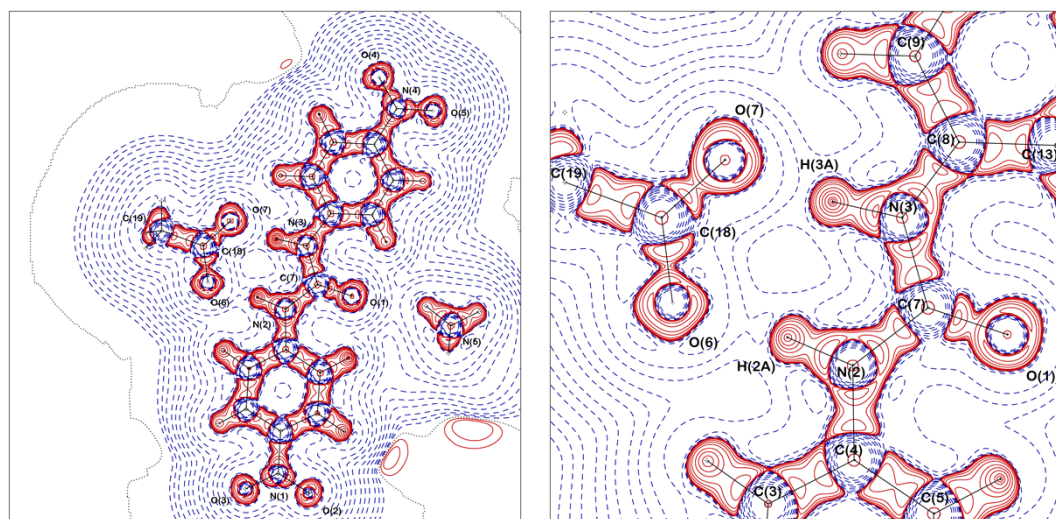


Figure S16: $-\nabla^2\rho(r)$ charge density distribution maps of whole receptor molecule (left) and anion binding region (right) of structure 5. Map drawn in the plane of the urea group.

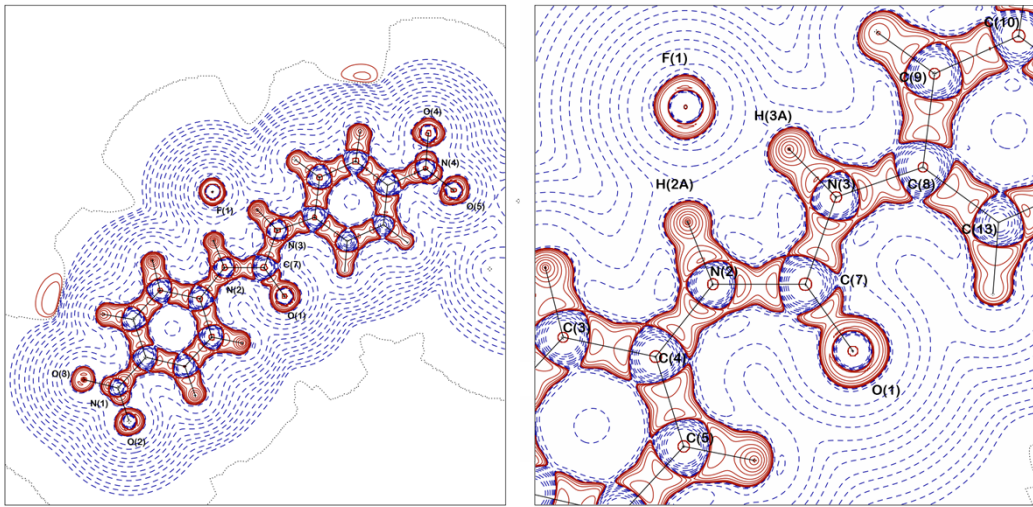


Figure S17: $-\nabla^2\rho(r)$ charge density distribution maps of whole receptor molecule (left) and anion binding region (right) of structure 6. Map drawn in the plane of the urea group.

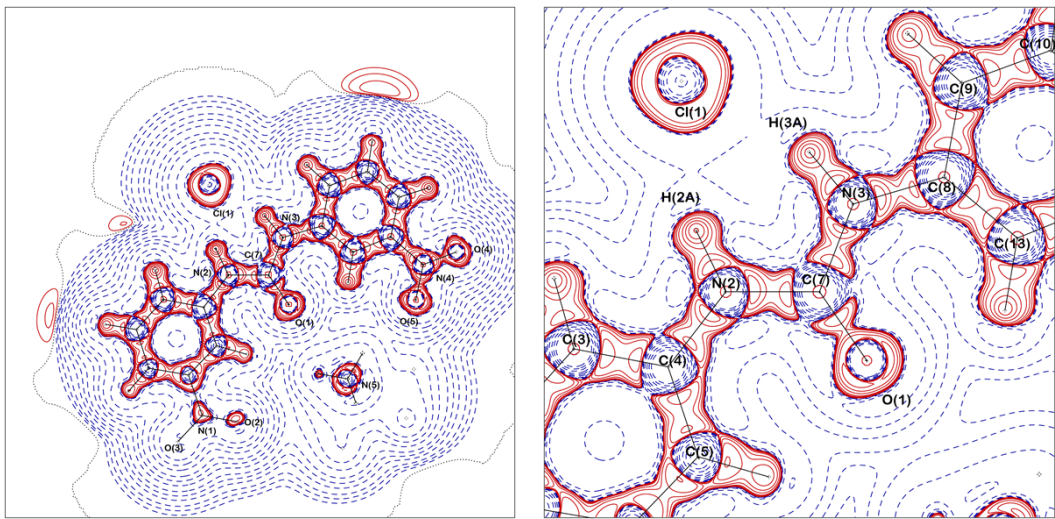


Figure S18: $-\nabla^2\rho(r)$ charge density distribution maps of whole receptor molecule (left) and anion binding region (right) of structure 7. Map drawn in the plane of the urea group.

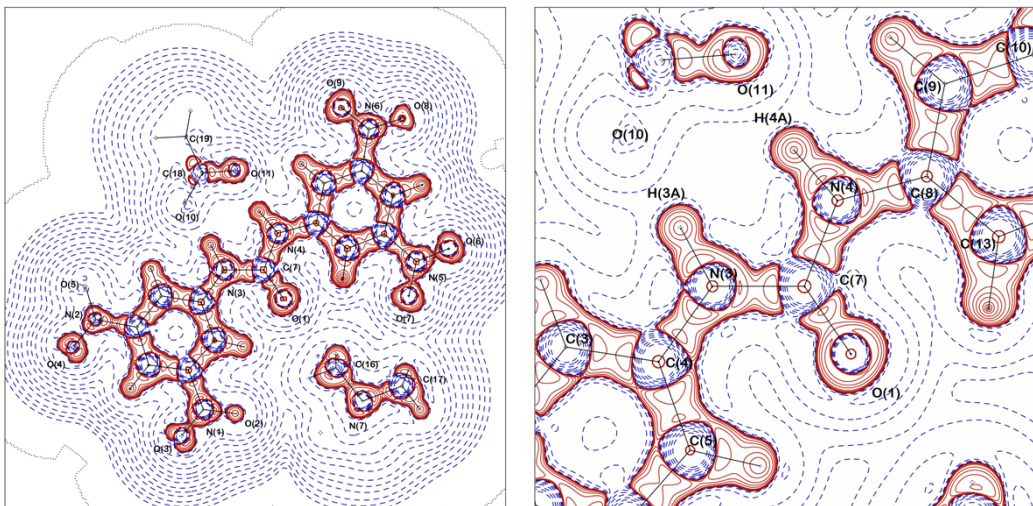


Figure S19: $-\nabla^2\rho(r)$ charge density distribution maps of whole receptor molecule (left) and anion binding region (right) of structure 8. Map drawn in the plane of the urea group.

- e. Bond path plots of structures **4 – 8**. Nuclear positions are displayed in blue, bond paths in yellow, BCPs in red, ring critical points green yellow and cage critical points in green copper.

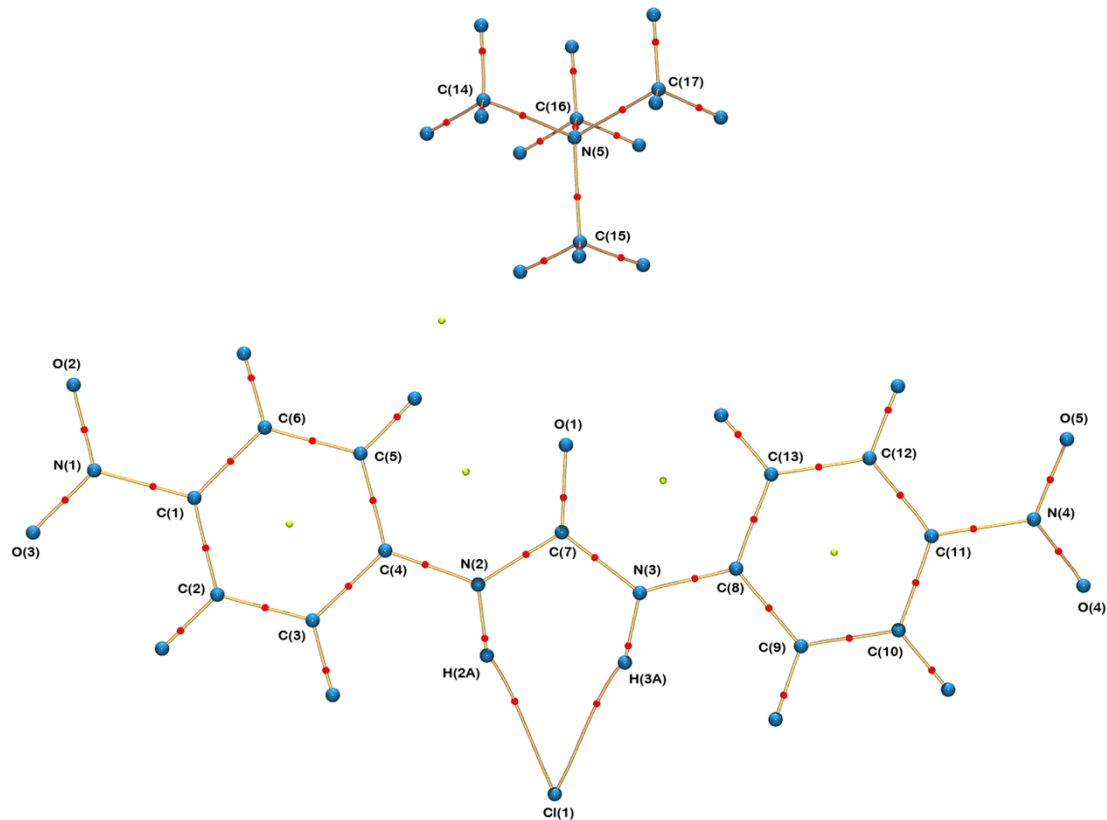


Figure S20: Bond path plot of structure **4** displaying the nuclear positions of the atoms in the structure, the bond paths (paths of maximum electron density linking these nuclear positions), and the position of the bond critical points (saddle points along the bond paths where electron density is at a minimum along the nuclear axis and at a maximum in the direction perpendicular to the molecular axis.).

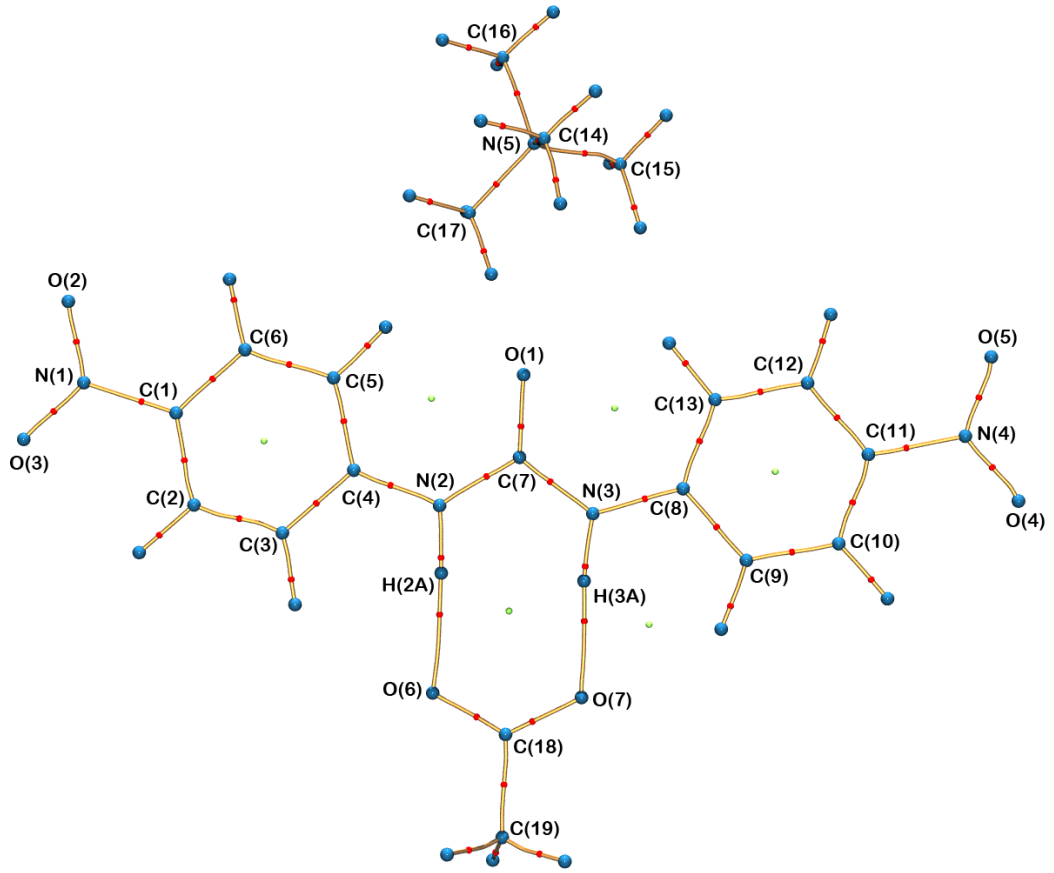


Figure S21: Bond path plot of structure 5 displaying the nuclear positions of the atoms in the structure, the bond paths and the position of the bond critical points.

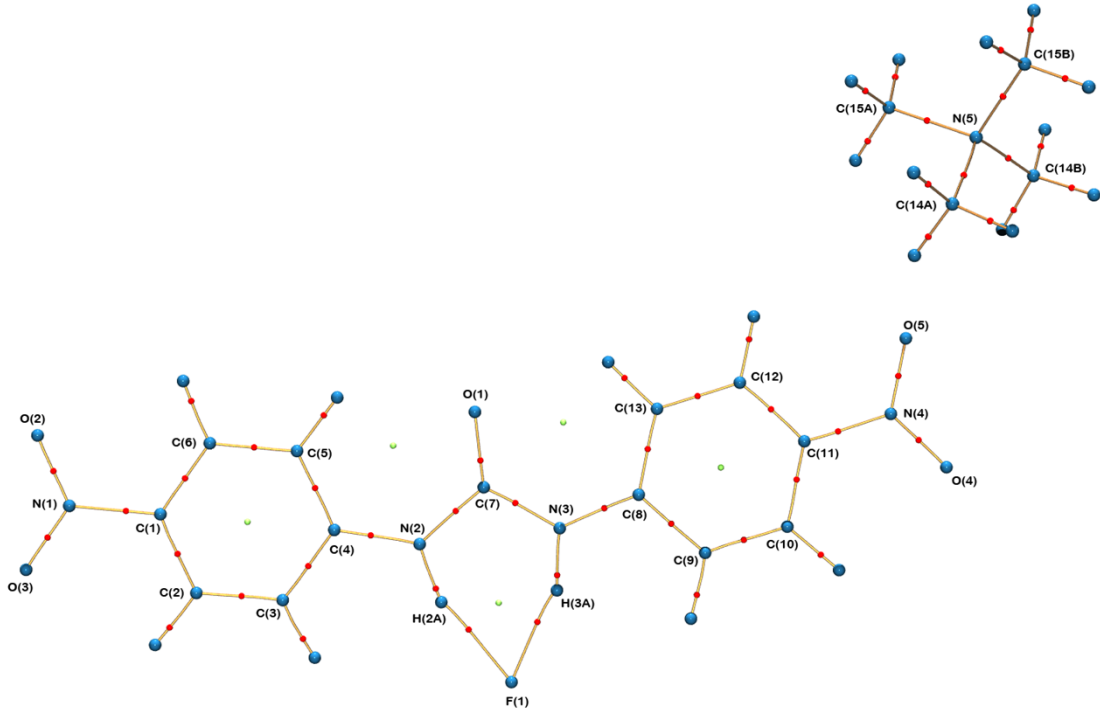


Figure S22: Bond path plot of structure 6 displaying the nuclear positions of the atoms in the structure, the bond paths and the position of the bond critical points.

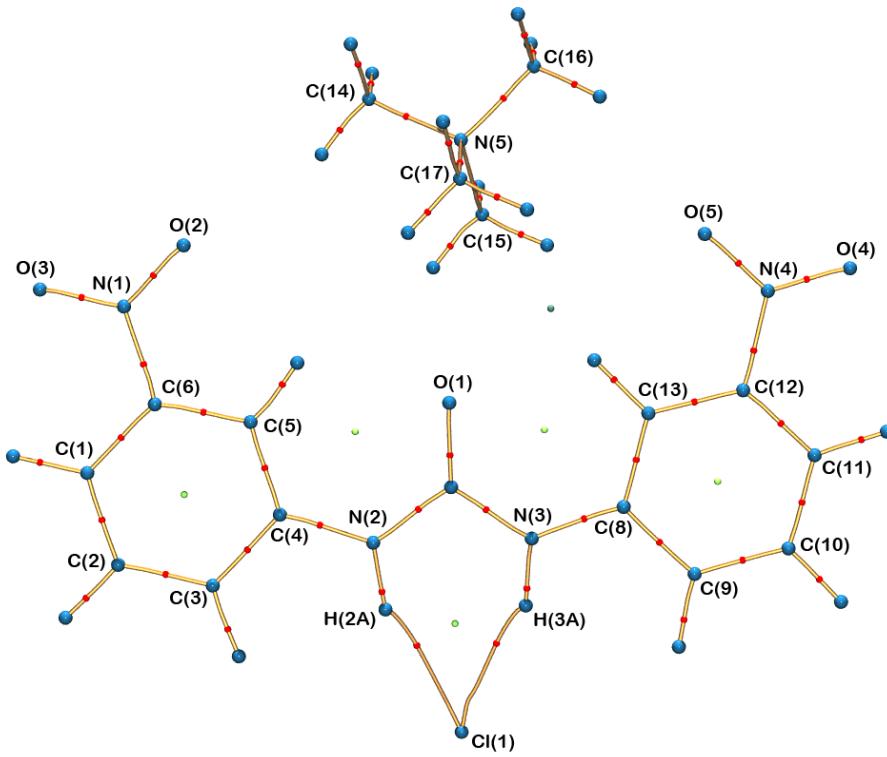


Figure S23: Bond path plot of structure 7 displaying the nuclear positions of the atoms in the structure, the bond paths and the position of the bond critical points.

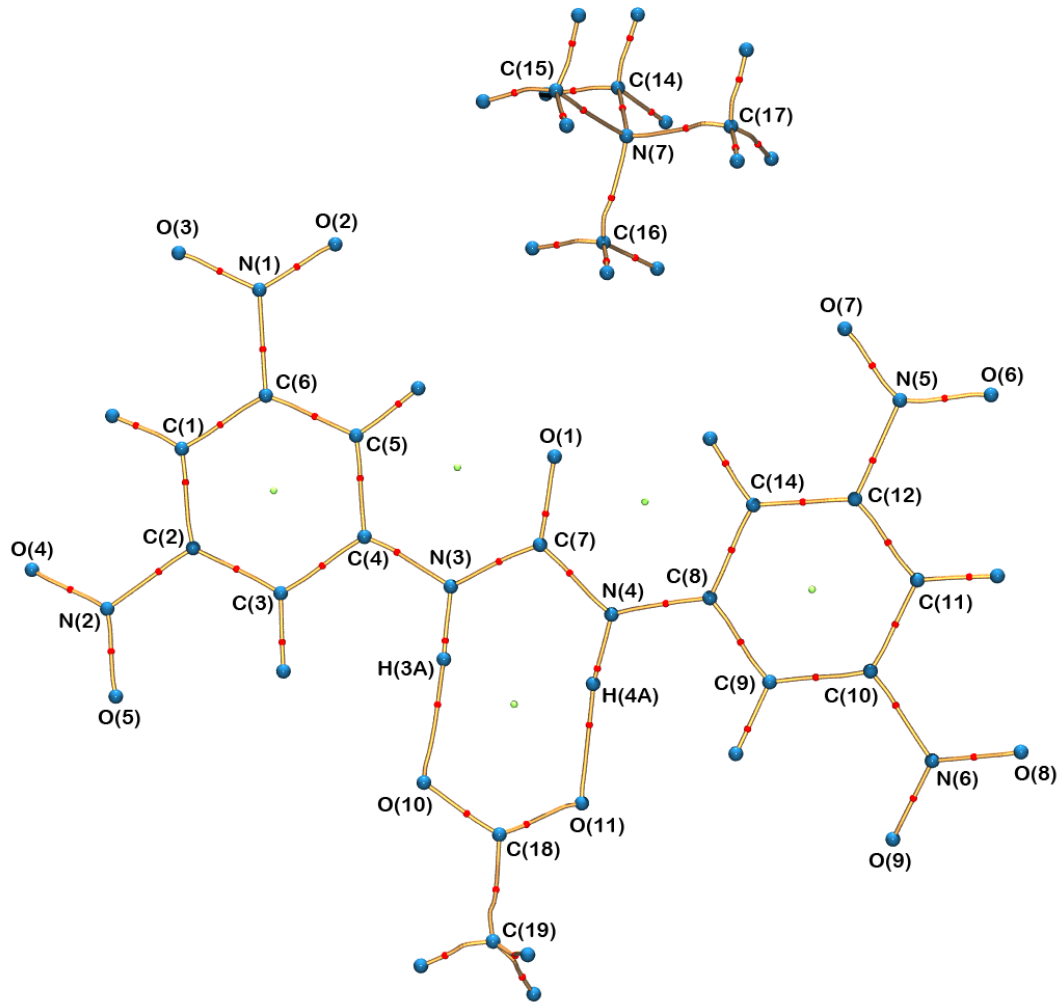


Figure S24: Bond path plot of structure **8** displaying the nuclear positions of the atoms in the structure, the bond paths and the position of the bond critical points.

3) Topological Properties of BCPs

- a. Electronic properties of the covalent bonds at the BCPs in the structures

Table S2: BCPs in structure 4

Bond	Electron Density ($e \text{ \AA}^{-3}$)	Laplacian ($e \text{ \AA}^{-5}$)	$R_{ij}(\text{\AA})$	$d_1(\text{\AA})$	$d_2(\text{\AA})$	λ_1	λ_2	λ_3	ε
O(1)-C(7)	3.07(4)	-39.1(2)	1.2237	0.7379	0.4859	-31.23	-25.99	18.09	0.20
O(2)-N(1)	3.36(3)	-10.1(1)	1.2377	0.6472	0.5905	-33.29	-29.95	53.11	0.11
O(3)-N(1)	3.40(4)	-11.0(2)	1.2314	0.6449	0.5865	-33.81	-30.44	53.27	0.11
O(5)-N(4)	3.29(4)	-3.2(2)	1.2411	0.6297	0.6114	-32.40	-26.36	55.54	0.23
O(4)-N(4)	3.29(3)	-3.3(1)	1.2404	0.6294	0.6110	-32.46	-26.39	55.56	0.23
N(1)-C(1)	1.83(3)	-13.43(9)	1.4505	0.8512	0.5993	-15.70	-12.20	14.48	0.29
N(2)-C(4)	2.10(3)	-17.13(9)	1.3867	0.7923	0.5944	-17.64	-15.20	15.72	0.16
N(2)-C(7)	2.17(3)	-19.0(1)	1.3851	0.7956	0.5896	-19.38	-15.61	15.95	0.24
N(2)-H(2A)	2.16(5)	-25.2(3)	1.0090	0.7647	0.2443	-29.46	-28.54	32.84	0.03
N(3)-C(7)	2.16(3)	-20.7(1)	1.3817	0.8010	0.5807	-19.43	-16.16	14.91	0.20
N(3)-C(8)	2.11(3)	-16.80(9)	1.3867	0.7936	0.5931	-17.57	-15.07	15.84	0.17
N(3)-H(3A)	2.22(5)	-29.7(3)	1.0090	0.7669	0.2421	-31.10	-30.08	31.47	0.03
N(5)-C(14)	1.62(3)	-6.61(8)	1.4984	0.8642	0.6343	-11.37	-10.91	15.67	0.04
N(5)-C(15)	1.66(3)	-5.89(8)	1.4956	0.8512	0.6443	-11.66	-10.98	16.75	0.06
N(5)-C(16)	1.70(3)	-7.09(8)	1.5012	0.8600	0.6412	-12.01	-11.94	16.86	0.01
N(5)-C(17)	1.63(3)	-6.99(8)	1.4969	0.8646	0.6323	-11.45	-11.16	15.61	0.03
N(4)-C(11)	1.85(3)	-13.07(9)	1.4532	0.8573	0.5959	-14.77	-13.02	14.71	0.13
C(1)-C(2)	2.18(2)	-18.48(6)	1.3969	0.7205	0.6764	-17.98	-14.12	13.61	0.27
C(1)-C(6)	2.15(2)	-18.02(6)	1.3957	0.7208	0.6749	-17.59	-13.86	13.43	0.27
C(2)-C(3)	2.16(2)	-17.46(6)	1.3840	0.6954	0.6886	-17.22	-13.83	13.59	0.24
C(2)-H(2)	1.88(4)	-17.1(1)	1.0830	0.7227	0.3604	-18.52	-17.82	19.27	0.04
C(3)-C(4)	2.10(2)	-16.97(6)	1.4119	0.6960	0.7159	-16.98	-13.62	13.63	0.25
C(3)-H(3)	1.83(4)	-16.6(1)	1.0830	0.7235	0.3595	-18.10	-17.20	18.67	0.05
C(4)-C(5)	2.07(2)	-17.35(6)	1.4083	0.7258	0.6825	-17.17	-13.39	13.21	0.28
C(5)-C(6)	2.14(2)	-17.50(6)	1.3898	0.6969	0.6929	-17.20	-13.84	13.53	0.24
C(5)-H(5)	1.86(4)	-18.5(1)	1.0831	0.7273	0.3558	-18.83	-17.74	18.09	0.06
C(6)-H(6)	1.83(4)	-16.2(1)	1.0831	0.7263	0.3567	-18.03	-17.29	19.10	0.04
C(8)-C(9)	2.08(2)	-16.70(6)	1.4130	0.7173	0.6957	-17.05	-13.18	13.52	0.29
C(8)-C(13)	2.08(2)	-17.12(6)	1.4093	0.7341	0.6751	-17.25	-13.22	13.35	0.30
C(9)-C(10)	2.19(3)	-19.11(7)	1.3838	0.6851	0.6987	-18.04	-14.33	13.25	0.26
C(9)-H(9)	1.86(4)	-18.9(1)	1.0830	0.7256	0.3574	-18.80	-17.81	17.74	0.06
C(10)-C(11)	2.15(3)	-17.19(7)	1.3983	0.7090	0.6893	-17.86	-13.28	13.94	0.35
C(10)-H(10)	1.83(4)	-17.5(1)	1.0830	0.7293	0.3537	-18.45	-17.64	1856	0.05
C(11)-C(12)	2.10(3)	-17.22(7)	1.3955	0.7211	0.6744	-17.19	-13.29	13.26	0.29
C(12)-C(13)	2.18(3)	-18.78(6)	1.3920	0.7194	0.6726	-17.62	-14.44	13.28	0.22
C(12)-H(12)	1.84(4)	-17.1(1)	1.0831	0.7223	0.3609	-18.39	-17.39	18.70	0.06
C(13)-H(13)	1.89(4)	-18.6(1)	1.0831	0.7256	0.3575	-19.06	-18.06	18.52	0.06
C(14)-H(14A)	1.92(4)	-16.7(1)	1.0592	0.6781	0.3811	-18.43	-17.39	19.08	0.06
C(14)-H(14B)	1.86(4)	-14.8(1)	1.0590	0.6921	0.3669	-18.03	-16.96	20.22	0.06
C(14)-H(14C)	1.91(4)	-16.7(1)	1.0591	0.6949	0.3642	-18.53	-17.84	19.66	0.04
C(15)-H(15A)	1.88(4)	-14.6(1)	1.0592	0.6842	0.3749	-17.92	-16.69	20.04	0.07
C(15)-H(15B)	1.84(5)	-13.9(1)	1.0592	0.6871	0.3721	-17.60	-16.34	20.02	0.08
C(15)-H(15C)	1.81(4)	-13.9(1)	1.0592	0.6405	0.4187	-16.02	-14.85	17.01	0.08
C(16)-H(16A)	1.89(4)	-15.7(1)	1.0591	0.6771	0.3821	-17.74	-17.20	19.29	0.03
C(16)-H(16B)	1.92(4)	-16.6(1)	1.0590	0.6991	0.3600	-18.89	-18.15	20.45	0.04

C(16)-H(16C)	1.88(4)	-16.0(1)	1.0591	0.6839	0.3751	-17.76	-17.22	19.02	0.03
C(17)-H(17A)	1.94(4)	-17.1(1)	1.0590	0.7061	0.3529	-19.22	-18.78	20.87	0.02
C(17)-H(17B)	1.88(4)	-16.0(1)	1.0592	0.6708	0.3884	-17.75	-16.87	18.61	0.05
C(17)-H(17C)	1.90(4)	-16.5(1)	1.0590	0.6863	0.3727	-18.35	-17.53	19.34	0.05

Table S3: BCPs in structure **5**

Bond	Electron Density ($e \text{ \AA}^{-3}$)	Laplacian ($e \text{ \AA}^{-5}$)	$R_{ij} (\text{\AA})$	$d_1 (\text{\AA})$	$d_2 (\text{\AA})$	λ_1	λ_2	λ_3	ϵ
O(1)-C(7)	3.02(5)	-48.5(3)	1.2299	0.7659	0.4640	-33.99	-26.47	11.96	0.28
O(4)-N(4)	3.51(5)	-16.1(2)	1.2348	0.628	0.6111	-35.73	-31.35	51.01	0.14
O(5)-N(4)	3.52(5)	-16.3(2)	1.2333	0.6232	0.6101	-35.83	-31.46	51.02	0.14
O(3)-N(1)	3.23(4)	-4.8(2)	1.2376	0.6113	0.6263	-29.52	-25.65	50.40	0.15
O(2)-N(1)	3.24(4)	-4.9(2)	1.2361	0.6107	0.6253	-29.60	-25.72	50.45	0.15
O(6)-C(18)	2.74(5)	-37.6(2)	1.2642	0.7786	0.4856	-26.86	-22.01	11.28	0.22
O(7)-C(18)	2.48(5)	-20.2(3)	1.2575	0.8251	0.4324	-23.02	-19.86	22.72	0.16
N(1)-C(1)	1.86(4)	-18.6(2)	1.4487	0.9012	0.5475	-15.07	-11.71	8.14	0.29
N(2)-C(4)	2.12(4)	-20.8(1)	1.3828	0.7930	0.5898	-18.09	-14.74	12.08	0.23
N(2)-C(7)	2.09(4)	-23.7(1)	1.3898	0.8200	0.5698	-18.83	-14.47	9.64	0.30
N(2)-H(2A)	1.90(6)	-22.7(3)	1.0443	0.7986	0.2457	-25.61	-24.60	27.52	0.04
N(3)-C(7)	2.28(4)	-26.3(1)	1.3726	0.7907	0.5818	-21.44	-16.41	11.56	0.31
N(3)-C(8)	1.99(4)	-17.3(1)	1.3871	0.8030	0.5841	-15.86	-13.19	11.72	0.20
N(3)-H(3A)	1.82(6)	-18.3(3)	1.0483	0.8108	0.2375	-24.90	-23.78	30.40	0.05
N(4)-C(11)	1.69(4)	-13.6(2)	1.4515	0.8932	0.5583	-12.30	-10.09	8.75	0.22
N(5)-C(14)	1.62(4)	-9.2(1)	1.5049	0.8764	0.6285	-11.05	-10.34	12.17	0.07
N(5)-C(15)	1.62(4)	-9.8(1)	1.4963	0.8602	0.6361	-12.37	-10.00	12.58	0.24
N(5)-C(16)	1.66(4)	-8.8(1)	1.4992	0.8650	0.6342	-12.01	-9.73	12.89	0.23
N(5)-C(17)	1.64(4)	-10.2(1)	1.4966	0.8779	0.6189	-11.29	-10.22	11.35	0.10
C(1)-C(2)	2.09(3)	-18.46(9)	1.4009	0.7041	0.6968	-16.55	-12.43	10.52	0.33
C(1)-C(6)	1.97(3)	-17.38(9)	1.3960	0.7384	0.6576	-14.80	-11.75	9.17	0.26
C(2)-C(3)	2.21(3)	-21.15(9)	1.3839	0.6828	0.7011	-17.31	-14.16	10.32	0.22
C(2)-H(2)	1.74(5)	-15.2(2)	1.0833	0.7092	0.3741	-15.89	-15.40	16.13	0.03
C(3)-C(4)	1.97(3)	-17.48(9)	1.4154	0.6840	0.7314	-14.95	-12.05	9.52	0.24
C(3)-H(3)	1.77(5)	-15.1(2)	1.1006	0.7396	0.3610	-17.28	-15.54	17.74	0.11
C(4)-C(5)	2.11(3)	-20.57(9)	1.4112	0.7319	0.6793	-16.99	-13.59	10.02	0.25
C(5)-C(6)	2.21(3)	-21.47(9)	1.3887	0.7036	0.6851	-17.29	-14.34	10.17	0.21
C(5)-H(5)	1.77(5)	-16.4(1)	1.1019	0.7215	0.3804	-16.90	-15.25	15.79	0.11
C(6)-H(6)	1.80(5)	-18.3(2)	1.1042	0.7630	0.3412	-18.17	-17.29	17.18	0.05
C(8)-C(9)	2.06(3)	-18.30(9)	1.4152	0.7378	0.6774	-16.35	-12.96	11.02	0.26
C(8)-C(13)	1.92(3)	-16.91(9)	1.4097	0.7347	0.6751	-15.25	-11.75	10.10	0.30
C(9)-C(10)	2.04(3)	-17.57(9)	1.3828	0.7006	0.6822	-15.55	-12.30	10.28	0.26
C(9)-H(9)	1.69(5)	-14.2(2)	1.1008	0.7517	0.3491	-16.59	-15.53	17.94	0.07
C(10)-C(11)	1.96(4)	-17.3(1)	1.3968	0.6391	0.7576	-15.59	-11.71	9.96	0.33
C(10)-H(10)	1.81(5)	-16.7(2)	1.0857	0.7161	0.3696	-17.55	-16.21	17.08	0.08
C(11)-C(12)	2.16(3)	-19.8(1)	1.3906	0.7006	0.6900	-16.97	-13.93	11.12	0.22
C(12)-C(13)	2.04(3)	-17.08(9)	1.3903	0.7112	0.6792	-15.36	-12.38	10.66	0.24
C(12)-H(12)	1.73(5)	-15.0(2)	1.0742	0.7225	0.3517	-16.59	-16.14	17.76	0.03
C(13)-H(13)	1.88(5)	-18.7(2)	1.0904	0.7272	0.3631	-18.56	-17.27	17.16	0.07
C(14)-H(14A)	1.86(5)	-18.3(2)	1.0702	0.7300	0.3402	-18.37	-17.78	17.84	0.03
C(14)-H(14B)	1.67(5)	-14.1(2)	1.1031	0.7343	0.3689	-15.20	-15.06	16.20	0.01
C(14)-H(14C)	1.68(6)	-13.4(2)	1.1125	0.7667	0.3458	-16.05	-15.88	18.48	0.01
C(15)-H(15A)	1.74(6)	-14.2(3)	1.0948	0.7903	0.3045	-18.21	-17.47	21.45	0.04
C(15)-H(15B)	1.78(5)	-16.5(1)	1.0817	0.6869	0.3949	-16.16	-15.54	15.20	0.04
C(15)-H(15C)	1.86(6)	-17.5(1)	1.1194	0.7134	0.4060	-16.85	-16.53	15.90	0.02
C(16)-H(16A)	1.83(5)	-15.9(2)	1.0969	0.7308	0.3661	-17.35	-17.05	18.54	0.02
C(16)-H(16B)	1.72(6)	-14.6(2)	1.0851	0.7564	0.3287	-17.16	-16.43	19.01	0.04

C(16)-H(16C)	1.80(5)	-17.8(1)	1.0885	0.6731	0.4154	-16.46	-15.03	13.67	0.09
C(17)-H(17A)	1.76(5)	-14.4(2)	1.0786	0.7065	0.3721	-16.34	-15.68	17.59	0.04
C(17)-H(17B)	1.75(5)	-14.9(2)	1.0725	0.7186	0.3539	-16.75	-16.17	18.00	0.04
C(17)-H(17C)	1.80(5)	-15.4(2)	1.0991	0.7480	0.3511	-17.23	-16.88	18.66	0.02
C(18)-C(19)	1.74(3)	-12.70(7)	1.5220	0.7579	0.7642	-12.98	-10.88	11.17	0.19
C(19)-H(19A)	1.77(5)	-15.1(1)	1.0934	0.7050	0.3884	-15.76	-15.46	16.09	0.02
C(19)-H(19B)	1.80(5)	-16.3(2)	1.0853	0.7470	0.3383	-17.71	-17.05	18.47	0.04
C(19)-H(19C)	1.64(5)	-12.8(2)	1.0748	0.7227	0.3521	-15.58	-14.72	17.48	0.06

Table S4: BCPs in structure **6**

Bond	Electron Density ($e \text{ \AA}^{-3}$)	Laplacian ($e \text{ \AA}^{-5}$)	$R_{ij} (\text{\AA})$	$d_1 (\text{\AA})$	$d_2 (\text{\AA})$	λ_1	λ_2	λ_3	ϵ
O(1)-C(7)	2.84(4)	-32.3(2)	1.2287	0.7886	0.4401	-27.89	-24.06	19.62	0.16
O(2)-N(1)	3.27(3)	-7.0(1)	1.2350	0.6226	0.6124	-30.16	-27.71	50.86	0.09
O(3)-N(1)	3.26(3)	-6.7(1)	1.2372	0.6234	0.6138	-29.97	-27.54	50.81	0.09
O(4)-N(4)	3.16(5)	-2.1(2)	1.2417	0.6227	0.6190	-29.29	-24.51	51.75	0.19
O(5)-N(4)	3.158(0)	-2.2(1)	1.2423	0.6231	0.6192	-29.29	-24.62	51.71	0.19
N(2)-C(4)	2.06(3)	-18.01(9)	1.3850	0.7954	0.5896	-16.68	-14.10	12.78	0.18
N(2)-C(7)	2.13(3)	-19.67(9)	1.3852	0.7938	0.5914	-17.54	-14.86	12.72	0.18
N(2)-H(2A)	2.05(5)	-23.3(3)	1.0092	0.7698	0.2394	-27.92	-27.52	32.15	0.01
N(3)-C(8)	2.11(3)	-18.5(9)	1.3765	0.7830	0.5935	-17.33	-14.48	13.32	0.20
N(3)-C(7)	2.09(3)	-22.2(1)	1.3858	0.8200	0.5659	-17.35	-14.95	10.18	0.16
N(3)-H(3A)	2.13(5)	-25.0(3)	1.0091	0.7632	0.2459	-28.83	-28.06	31.85	0.03
N(1)-C(1)	1.72(3)	-12.8(1)	1.4508	0.9020	0.5488	-12.15	-10.12	9.42	0.20
N(4)-C(11)	1.80(3)	-14.0(1)	1.4486	0.8859	0.5627	-13.71	-10.61	10.29	0.29
N(5)-C(15A)	1.782(0)	-10.466(0)	1.4958	0.8390	0.6568	-12.70	-12.68	14.91	0.00
N(5)-C(14A)	1.748(0)	-9.477(0)	1.5027	0.8392	0.6635	-12.35	-12.25	15.12	0.01
N(5)-C(15B)	1.778(0)	-10.331(0)	1.4968	0.8392	0.6576	-12.65	-12.61	14.93	0.00
N(5)-C(14B)	1.762(0)	-9.947(0)	1.4977	0.8378	0.6599	-12.59	-12.41	15.06	0.01
C(5)-C(4)	2.03(2)	-16.72(6)	1.4086	0.6632	0.7452	-15.52	-12.19	10.99	0.27
C(5)-C(6)	2.09(2)	-18.35(6)	1.3915	0.6841	0.7074	-16.39	-12.84	10.89	0.28
C(5)-H(5)	1.84(4)	-17.3(1)	1.0831	0.7215	0.3617	-17.64	-17.14	17.51	0.03
C(4)-C(3)	2.04(2)	-17.07(5)	1.4167	0.7240	0.6928	-15.88	-12.52	11.34	0.27
C(1)-C(6)	2.06(2)	-17.91(6)	1.3971	0.7037	0.6934	-16.07	-12.74	10.91	0.26
C(1)-C(2)	2.08(2)	-17.85(6)	1.4000	0.6971	0.7029	-16.05	-12.96	11.16	0.24
C(3)-C(2)	2.13(2)	-19.86(6)	1.3847	0.6611	0.7236	-16.75	-13.47	10.36	0.24
C(3)-H(3)	1.77(3)	-16.3(1)	1.0840	0.7151	0.3688	-16.98	-16.22	16.93	0.05
C(6)-H(6)	1.85(4)	-17.0(1)	1.0832	0.7386	0.3446	-18.55	-17.69	19.22	0.05
C(2)-H(2)	1.86(3)	-18.8(1)	1.0832	0.7142	0.3690	-18.11	-17.06	16.34	0.06
C(8)-C(9)	2.02(2)	-17.11(6)	1.4169	0.6986	0.7183	-15.60	-12.56	11.05	0.24
C(8)-C(13)	2.00(2)	-17.56(6)	1.4120	0.7482	0.6638	-15.69	-12.28	10.42	0.28
C(11)-C(12)	2.15(3)	-18.97(7)	1.3991	0.7395	0.6597	-16.50	-13.41	10.95	0.23
C(11)-C(10)	2.09(3)	-20.26(8)	1.4000	0.6293	0.7707	-16.65	-13.00	9.39	0.28
C(9)-C(10)	2.17(3)	-19.67(7)	1.3826	0.6538	0.7288	-17.21	-12.97	10.52	0.33
C(9)-H(9)	1.74(4)	-15.1(1)	1.0837	0.6898	0.3939	-15.93	-14.97	15.80	0.06
C(13)-C(12)	2.11(2)	-18.10(6)	1.3906	0.6814	0.7092	-16.47	-12.68	11.06	0.30
C(13)-H(13)	1.78(4)	-16.6(1)	1.0831	0.7188	0.3643	-16.99	-16.42	16.83	0.03
C(12)-H(12)	1.85(4)	-17.6(1)	1.0832	0.7105	0.3728	-17.70	-16.64	16.78	0.06
C(10)-H(10)	1.87(4)	-19.8(1)	1.0832	0.7016	0.3816	-18.57	-16.79	15.51	0.11
C(15)-H(15A)	1.876(0)	-18.277(0)	1.0590	0.6711	0.3879	-16.93	-16.26	14.91	0.04
C(15)-H(15B)	1.875(0)	-18.280(0)	1.0590	0.6711	0.3879	-16.93	-16.26	14.92	0.04
C(15)-H(15C)	1.875(0)	-18.284(0)	1.0590	0.6711	0.3879	-16.94	-16.26	14.92	0.04
C(14)-H(14A)	1.876(0)	-18.276(0)	1.0590	0.6711	0.3879	-16.92	-16.26	14.91	0.04
C(14)-H(14B)	1.875(0)	-18.278(0)	1.0590	0.6711	0.3879	-16.93	-16.26	14.91	0.04
C(14)-H(14C)	1.874(0)	-18.291(0)	1.0590	0.6708	0.3882	-16.94	-16.24	14.89	0.04

C(15B)-H(15D)	1.875 (0)	-18.282(0)	1.0590	0.6711	0.3879	-16.93	-16.26	14.91	0.04
C(15B)-H(15E)	1.876(0)	-18.275(0)	1.0590	0.6711	0.3879	-16.93	-16.26	14.91	0.04
C(15B)-H(15F)	1.875(0)	-18.283(0)	1.0590	0.6711	0.3879	-16.93	-16.26	14.92	0.04
C(14B)-H(14D)	1.874 (0)	-18.292(0)	1.0590	0.6709	0.3881	-16.94	-16.25	14.90	0.04
C(14B)-H(14E)	1.876(0)	-18.275(0)	1.0590	0.6712	0.3878	-16.92	-16.27	14.92	0.04
C(14B)-H(14F)	1.875(0)	-18.289(0)	1.0590	0.6710	0.3880	-16.94	-16.25	14.90	0.04

Table S5: BCPs in structure 7

Bond	Electron Density ($e \text{ \AA}^{-3}$)	Laplacian ($e \text{ \AA}^{-5}$)	$R_{ij}(\text{\AA})$	$d_1(\text{\AA})$	$d_2(\text{\AA})$	λ_1	λ_2	λ_3	ϵ
O(1)-C(7)	2.86(5)	-35.9(2)	1.2257	0.7570	0.4687	-28.05	-23.45	15.64	0.20
O(2)-N(1)	3.25(4)	-4.7(2)	1.2300	0.6126	0.6174	-31.14	-26.81	53.28	0.16
O(3)-N(1)	3.27(4)	-5.0(2)	1.2268	0.6115	0.6153	-31.40	-26.96	53.40	0.16
O(4)-N(4)	3.35(4)	-14.2(2)	1.2223	0.6418	0.5805	-34.64	-29.04	49.49	0.19
O(5)-N(4)	3.31(4)	-13.3(2)	1.2279	0.6437	0.5841	-34.13	-28.62	49.43	0.19
N(1)-C(6)	1.65(4)	-9.1(1)	1.4705	0.8797	0.5909	-11.62	-10.86	13.35	0.07
N(2)-C(4)	2.03(4)	-17.0(1)	1.3934	0.8104	0.5830	-16.56	-14.57	14.11	0.14
N(2)-C(7)	2.20(4)	-21.2(1)	1.3746	0.8035	0.5712	-18.92	-15.96	13.65	0.19
N(2)-H(2A)	2.02(6)	-27.0(4)	1.0244	0.7806	0.2438	-28.30	-26.84	28.17	0.05
N(3)-C(7)	2.08(4)	-16.1(1)	1.3788	0.7768	0.6020	-17.81	-13.89	15.57	0.28
N(3)-C(8)	2.03(4)	-16.4(1)	1.3930	0.8018	0.5912	-16.83	-14.06	14.54	0.20
N(3)-H(3A)	2.13(6)	-25.7(3)	1.0117	0.7616	0.2500	-29.12	-27.47	30.93	0.06
N(4)-C(12)	1.71(4)	-10.7(1)	1.4666	0.8730	0.5936	-12.61	-11.39	13.32	0.11
N(5)-C(14)	1.55(5)	-8.2(2)	1.4892	0.8985	0.5908	-9.70	-9.30	10.81	0.04
N(5)-C(15)	1.54(4)	-6.7(1)	1.4947	0.8734	0.6213	-10.57	-8.99	12.81	0.17
N(5)-C(16)	1.59(4)	-6.1(1)	1.4986	0.8661	0.6324	-10.49	-9.43	13.79	0.11
N(5)-C(17)	1.59(4)	-7.3(1)	1.4955	0.8681	0.6274	-11.24	-9.38	13.34	0.20
C(1)-C(2)	2.04(4)	-16.4(1)	1.3937	0.7051	0.6886	-16.02	-12.80	12.42	0.25
C(1)-C(6)	2.13(4)	-16.6(1)	1.3892	0.7058	0.6833	-16.75	-13.28	13.39	0.26
C(1)-H(1)	1.81(6)	-15.2(2)	1.0863	0.7372	0.3491	-18.06	-17.14	19.99	0.05
C(2)-C(3)	2.14(4)	-16.86(9)	1.3884	0.7001	0.6883	-16.89	-13.16	13.19	0.28
C(2)-H(2)	1.87(6)	-15.5(2)	1.0643	0.6991	0.3652	-18.29	-17.04	19.86	0.07
C(3)-C(4)	2.07(3)	-16.53(8)	1.4059	0.7071	0.6988	-16.34	-13.18	12.99	0.24
C(3)-H(3)	1.78(6)	-15.6(2)	1.0771	0.7179	0.3593	-17.30	-16.65	18.33	0.04
C(4)-C(5)	2.04(3)	-16.60(9)	1.3977	0.7064	0.6913	-15.86	-13.11	12.37	0.21
C(5)-C(6)	2.06(4)	-15.50(9)	1.3918	0.6910	0.7008	-15.73	-12.95	13.19	0.21
C(5)-H(5)	1.83(6)	-17.1(2)	1.0911	0.7463	0.3448	-18.58	-17.63	19.11	0.05
C(8)-C(9)	1.95(3)	-14.22(8)	1.4064	0.7146	0.6918	-14.93	-11.81	12.52	0.26
C(8)-C(13)	2.05(3)	-16.11(9)	1.3972	0.7050	0.6922	-16.04	-12.65	12.57	0.27
C(9)-C(10)	2.10(4)	-16.79(9)	1.3901	0.7022	0.6880	-16.49	-13.26	12.96	0.24
C(9)-H(9)	1.75(6)	-14.5(2)	1.0664	0.7081	0.3583	-16.88	-16.39	18.74	0.03
C(10)-C(11)	2.04(4)	-16.26(9)	1.3939	0.6971	0.6968	-15.90	-12.88	12.52	0.23
C(10)-H(10)	1.83(6)	-16.3(2)	1.0784	0.7029	0.3754	-17.57	-16.78	18.04	0.05
C(11)-C(12)	2.14(4)	-18.3(1)	1.3884	0.6760	0.7124	-16.83	-14.02	12.53	0.20
C(11)-H(11)	1.77(5)	-14.0(2)	1.0780	0.7366	0.3414	-17.75	-16.78	20.56	0.06
C(12)-C(13)	2.10(4)	-17.96(9)	1.3891	0.7220	0.6670	-16.87	-13.42	12.34	0.26
C(13)-H(13)	1.85(6)	-17.8(2)	1.0877	0.7282	0.3595	-18.34	-17.26	17.81	0.06
C(14)-H(14A)	1.74(7)	-12.9(2)	1.0782	0.7154	0.3628	-16.51	-15.17	18.76	0.09
C(14)-H(14B)	1.78(7)	-15.4(2)	1.1013	0.7395	0.3618	-17.01	-16.14	17.80	0.05
C(14)-H(14C)	1.73(7)	-12.5(2)	1.1043	0.7507	0.3536	-16.58	-15.51	19.58	0.07
C(15)-H(15A)	1.72(7)	-13.4(2)	1.0868	0.7223	0.3645	-15.95	-15.70	18.28	0.02
C(15)-H(15B)	1.83(6)	-14.5(2)	1.0892	0.7127	0.3765	-17.17	-16.09	18.72	0.07
C(15)-H(15C)	1.76(7)	-12.9(2)	1.0778	0.7220	0.3558	-16.71	-15.65	19.44	0.07
C(16)-H(16A)	1.78(7)	-13.6(2)	1.0750	0.6930	0.3820	-16.80	-14.70	17.88	0.14

C(16)-H(16B)	1.81(6)	-15.4(2)	1.1089	0.7063	0.4026	-16.98	-14.84	16.42	0.14
C(16)-H(16C)	1.66(7)	-10.2(2)	1.0694	0.6902	0.3792	-14.66	-13.66	18.11	0.07
C(17)-H(17A)	1.76(6)	-13.1(2)	1.1172	0.7557	0.3616	-17.07	-15.41	19.38	0.11
C(17)-H(17B)	1.68(8)	-12.0(2)	1.0434	0.6063	0.4371	-13.40	-12.57	13.66	0.09
C(17)-H(17C)	1.84(7)	-14.6(2)	1.0867	0.7274	0.3593	-17.85	-16.03	19.30	0.11

Table S6: BCPs in structure **8**

Bond	Electron Density ($e \text{ \AA}^{-3}$)	Laplacian ($e \text{ \AA}^{-5}$)	R_{ij} (\text{\AA})	d_1 (\text{\AA})	d_2 (\text{\AA})	λ_1	λ_2	λ_3	ε
O(1)-C(7)	2.89(6)	-45.2(3)	1.2323	0.7912	0.4411	-32.03	-27.90	14.75	0.15
O(2)-N(1)	3.41(5)	-12.3(2)	1.2343	0.6209	0.6134	-32.33	-29.29	49.34	0.10
O(3)-N(1)	3.48(5)	-13.8(2)	1.2247	0.6176	0.6070	-33.17	-30.09	49.42	0.10
O(4)-N(2)	3.35(4)	-10.9(2)	1.2299	0.6308	0.5992	-30.46	-28.74	48.27	0.06
O(5)-N(2)	3.31(5)	-10.1(2)	1.2354	0.6326	0.6028	-30.03	-28.31	48.24	0.06
O(6)-N(5)	3.32(4)	-10.6(2)	1.2279	0.6252	0.6027	-30.78	-28.06	48.28	0.10
O(7)-N(5)	3.35(4)	-11.1(2)	1.2232	0.6235	0.5997	-31.07	-28.32	48.33	0.10
O(8)-N(6)	3.29(4)	-13.6(2)	1.2313	0.6481	0.5832	-30.81	-27.99	45.22	0.10
O(9)-N(6)	3.30(5)	-13.9(2)	1.2295	0.6475	0.5820	-30.95	-28.16	45.20	0.10
O(10)-C(18)	3.16(5)	-44.4(2)	1.2562	0.7257	0.5305	-31.10	-26.92	13.60	0.16
O(11)-C(18)	2.64(6)	-27.8(3)	1.2676	0.8486	0.4190	-29.40	-28.27	29.85	0.04
N(3)-C(4)	2.02(5)	-25.7(2)	1.3903	0.8980	0.4923	-17.28	-14.62	6.21	0.18
N(3)-C(7)	2.16(4)	-19.6(1)	1.3807	0.7640	0.6167	-17.75	-14.91	13.09	0.19
N(3)-H(3A)	2.02(8)	-19.0(4)	1.0092	0.7561	0.2531	-26.40	-25.81	33.18	0.02
N(1)-C(6)	1.79(4)	-14.4(1)	1.4738	0.8250	0.6488	-13.65	-12.44	11.69	0.10
N(2)-C(2)	1.72(4)	-16.3(1)	1.4714	0.8884	0.5829	-12.89	-11.13	7.74	0.16
N(4)-C(7)	2.26(4)	-29.0(1)	1.3752	0.8108	0.5644	-20.27	-17.47	8.74	0.16
N(4)-C(8)	2.08(4)	-19.5(1)	1.3878	0.7730	0.6148	-17.46	-14.49	12.50	0.21
N(4)-H(4A)	1.98(8)	-19.6(5)	1.0095	0.7757	0.2338	-26.91	-26.59	33.87	0.01
N(5)-C(12)	1.78(4)	-16.5(1)	1.4739	0.8908	0.5832	-13.70	-11.31	8.49	0.21
N(6)-C(10)	1.78(4)	-17.0(1)	1.4719	0.8951	0.5768	-13.28	-12.07	8.37	0.10
N(7)-C(14)	1.46(4)	-9.5(1)	1.5002	0.8883	0.6120	-8.99	-7.60	7.07	0.18
N(7)-C(15)	1.55(5)	-12.2(2)	1.4881	0.9110	0.5772	-10.12	-8.23	6.13	0.23
N(7)-C(16)	1.60(5)	-8.7(1)	1.5013	0.8862	0.6151	-11.21	-7.15	9.64	0.57
N(7)-C(17)	1.55(5)	-8.1(1)	1.5027	0.8888	0.6139	-10.37	-8.55	10.85	0.21
C(1)-C(6)	2.14(4)	-20.0(1)	1.3924	0.6449	0.7475	-15.28	-13.43	8.66	0.14
C(1)-C(2)	1.98(6)	-14.6(3)	1.3946	0.4685	0.9262	-11.73	-11.04	8.18	0.06
C(1)-H(1)	1.81(6)	-15.2(2)	1.0836	0.7287	0.3550	-17.05	-16.27	18.13	0.05
C(6)-C(5)	2.13(4)	-21.0(1)	1.3893	0.7425	0.6468	-16.54	-13.01	8.56	0.27
C(5)-C(4)	1.96(4)	-19.3(1)	1.4088	0.6010	0.8078	-13.52	-12.61	6.88	0.07
C(5)-H(5)	1.86(7)	-18.1(2)	1.0832	0.7377	0.3455	-17.81	-17.54	17.29	0.02
C(4)-C(3)	2.05(4)	-18.95(9)	1.4078	0.7059	0.7019	-15.41	-12.77	9.24	0.21
C(3)-C(2)	2.22(4)	-23.12(9)	1.3853	0.7170	0.6683	-17.87	-13.86	8.61	0.29
C(3)-H(3)	1.79(6)	-17.3(2)	1.0835	0.7051	0.3784	-16.47	-16.05	15.18	0.03
C(8)-C(13)	2.06(4)	-19.40(9)	1.4056	0.7136	0.6920	-15.49	-12.96	9.04	0.20
C(8)-C(9)	2.04(4)	-19.45(8)	1.4099	0.7384	0.6714	-15.43	-13.05	9.03	0.18
C(13)-C(12)	2.17(4)	-20.86(9)	1.3919	0.6833	0.7085	-16.69	-13.73	9.56	0.22
C(13)-H(13)	1.86(6)	-17.1(2)	1.0835	0.6862	0.3973	-16.44	-16.09	15.48	0.02
C(12)-C(11)	2.14(4)	-21.8(1)	1.3861	0.7359	0.6501	-16.60	-13.73	8.53	0.21
C(11)-C(10)	2.16(4)	-21.6(1)	1.3937	0.6701	0.7236	-16.47	-14.00	8.83	0.18
C(11)-H(11)	1.91(6)	-18.3(2)	1.0830	0.7155	0.3675	-18.31	-17.40	17.42	0.05
C(10)-C(9)	2.18(4)	-22.2(1)	1.3833	0.7481	0.6351	-16.79	-13.79	8.38	0.22
C(9)-H(9)	1.87(6)	-17.5(2)	1.0830	0.7084	0.3746	-17.11	-16.92	16.53	0.01
C(14)-H(14A)	1.76(7)	-15.4(3)	1.0592	0.7332	0.3260	-17.28	-16.57	18.43	0.04

C(14)-H(14B)	1.79(7)	-17.0(2)	1.0599	0.7061	0.3538	-16.95	-15.89	15.82	0.07
C(14)-H(14C)	1.82(7)	-17.1(2)	1.0598	0.6850	0.3748	-16.30	-15.93	15.12	0.02
C(15)-H(15A)	2.05(9)	-22.0(4)	1.0630	0.7444	0.3186	-22.02	-20.11	20.12	0.09
C(15)-H(15B)	1.82(9)	-21.9(4)	1.0591	0.7652	0.2939	-20.67	-18.38	17.15	0.12
C(15)-H(15C)	1.90(8)	-26.0(2)	1.0666	0.6490	0.4177	-20.43	-15.30	9.77	0.34
C(16)-H(16A)	1.73(6)	-15.6(2)	1.0610	0.6588	0.4021	-14.78	-13.89	13.03	0.06
C(16)-H(16B)	1.72(8)	-13.52(3)	1.0619	0.7190	0.3428	-16.74	-14.74	17.96	0.14
C(16)-H(16C)	1.73(7)	-15.8(2)	1.0594	0.6657	0.3937	-15.09	-13.64	12.89	0.11
C(17)-H(17A)	1.53(7)	-11.8(2)	1.0606	0.6200	0.4406	-11.71	-10.45	10.39	0.12
C(17)-H(17B)	1.75(7)	-15.0(2)	1.0591	0.6475	0.4116	-15.43	-11.99	12.41	0.29
C(17)-H(17C)	1.66(8)	-11.1(3)	1.0599	0.6976	0.3623	-15.34	-12.74	17.02	0.20
C(18)-C(19)	1.64(4)	-13.07(9)	1.5096	0.7918	0.7178	-10.34	-8.09	5.35	0.28
C(19)-H(19A)	1.57(8)	-17.9(4)	1.0606	0.7955	0.2651	-16.40	-15.07	13.54	0.09
C(19)-H(19B)	1.60(8)	-12.4(4)	1.0610	0.7658	0.2952	-14.60	-13.72	15.88	0.06
C(19)-H(19C)	1.34(8)	-10.3(2)	1.0718	0.6607	0.4111	-9.34	-7.20	6.26	0.30

b. Bond ellipticity profiles of the aromatic bond paths in the structures

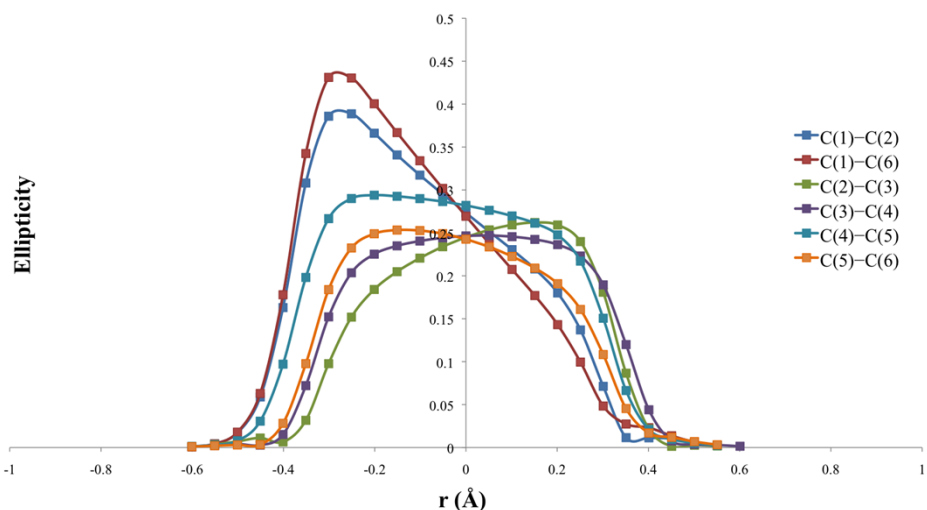


Figure S25: Graph of bond ellipticity along the bond paths for phenyl ring C(1)-C(6) in 4

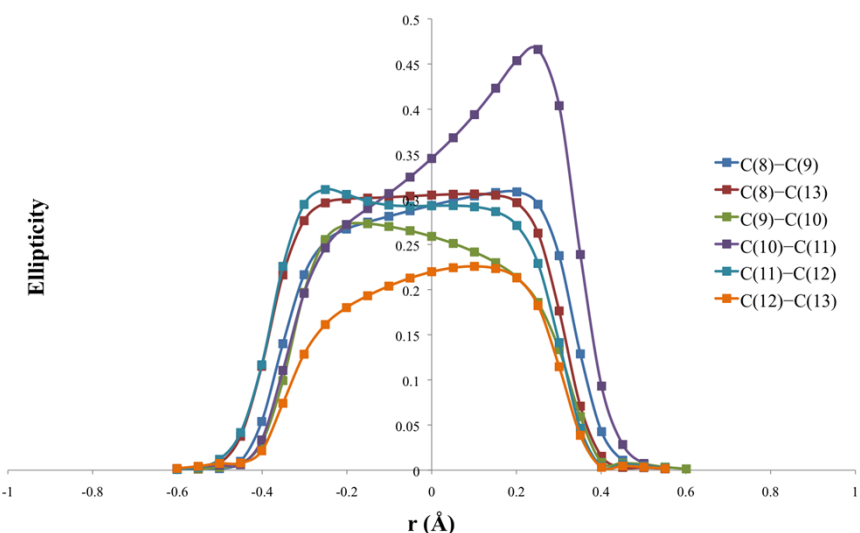


Figure S26: Graph of bond ellipticity along the bond paths for phenyl ring C(8)-C(13) in 4

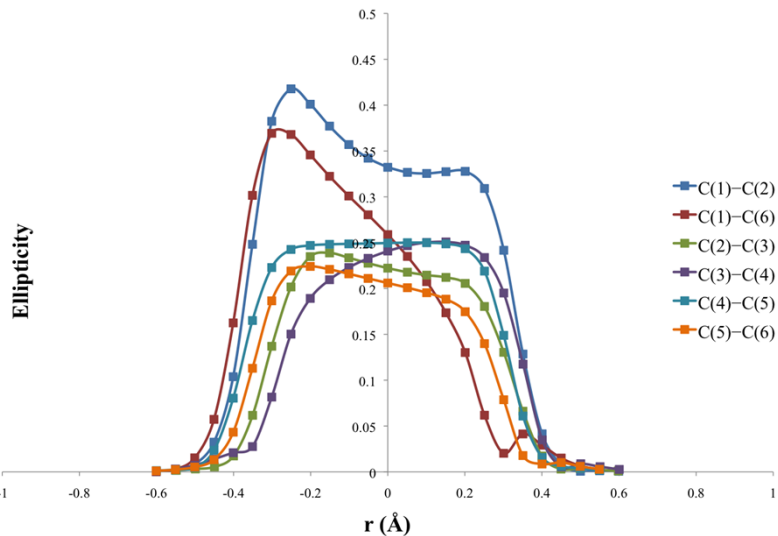


Figure S27: Graph of bond ellipticity along the bond paths for phenyl ring C(1)–C(6) in **5**

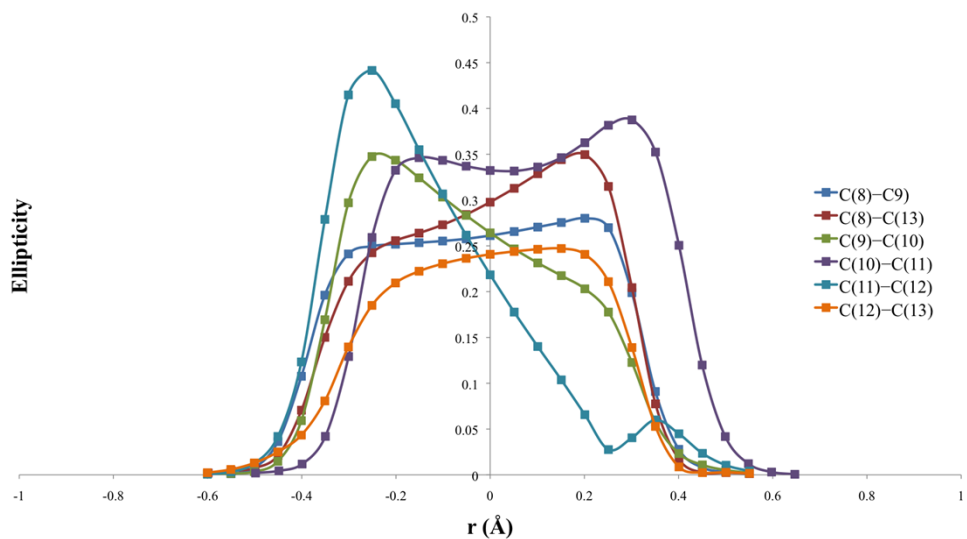


Figure S28: Graph of bond ellipticity along the bond paths for phenyl ring C(8)–C(13) in **5**

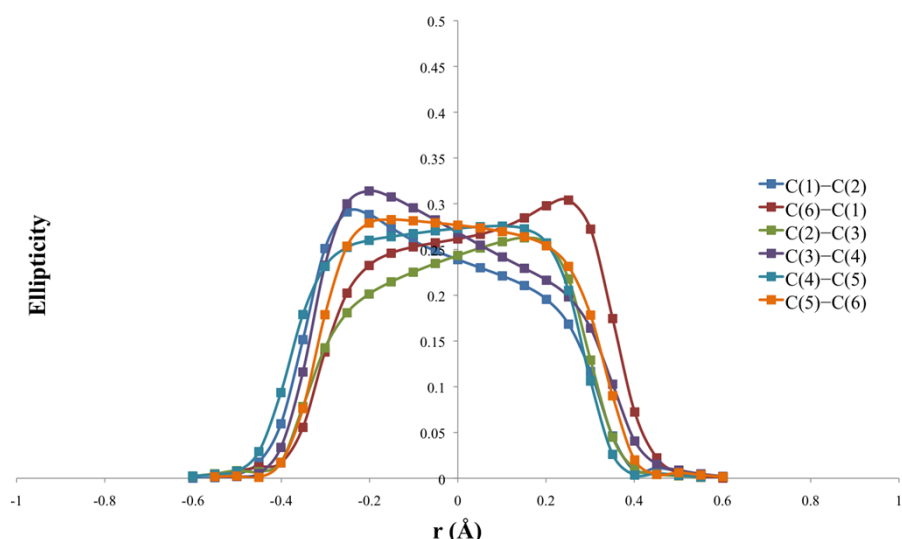


Figure S29: Graph of bond ellipticity along the bond paths for phenyl ring C(1)–C(6) in **6**

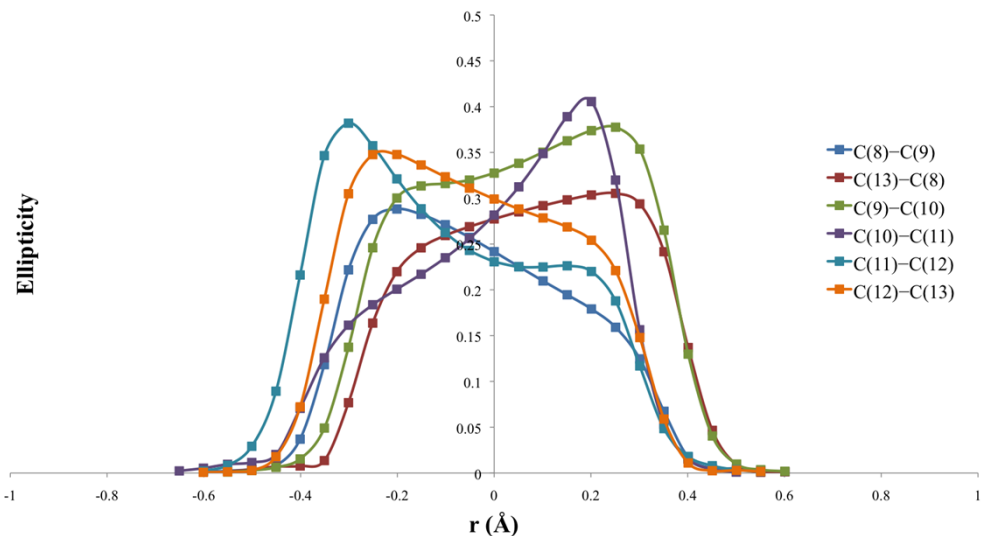


Figure S30: Graph of bond ellipticity along the bond paths for phenyl ring C(8)–C(13) in **6**

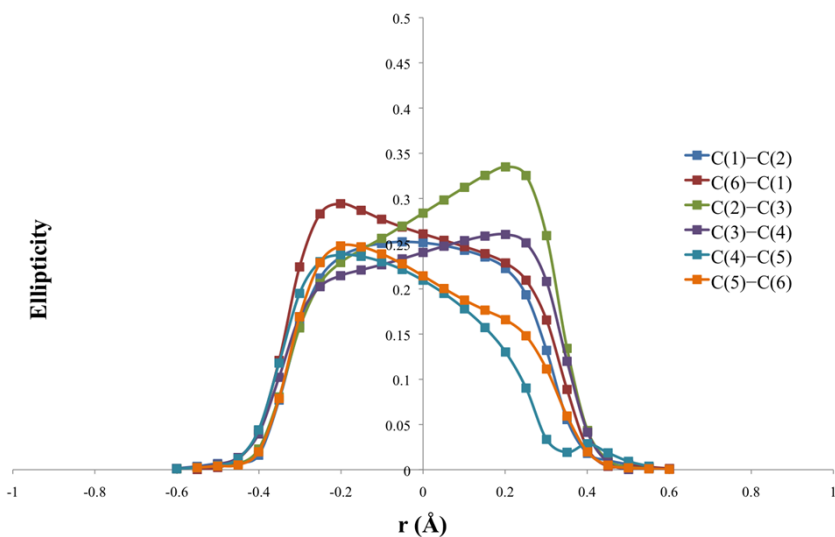


Figure S31: Graph of bond ellipticity along the bond paths for phenyl ring C(1)–C(6) in **7**

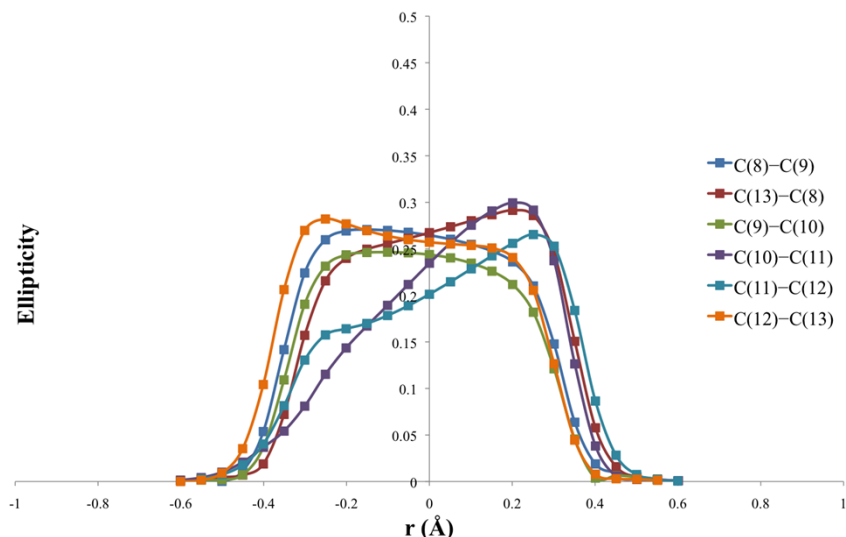


Figure S32: Graph of bond ellipticity along the bond paths for phenyl ring C(8)–C(13) in **7**

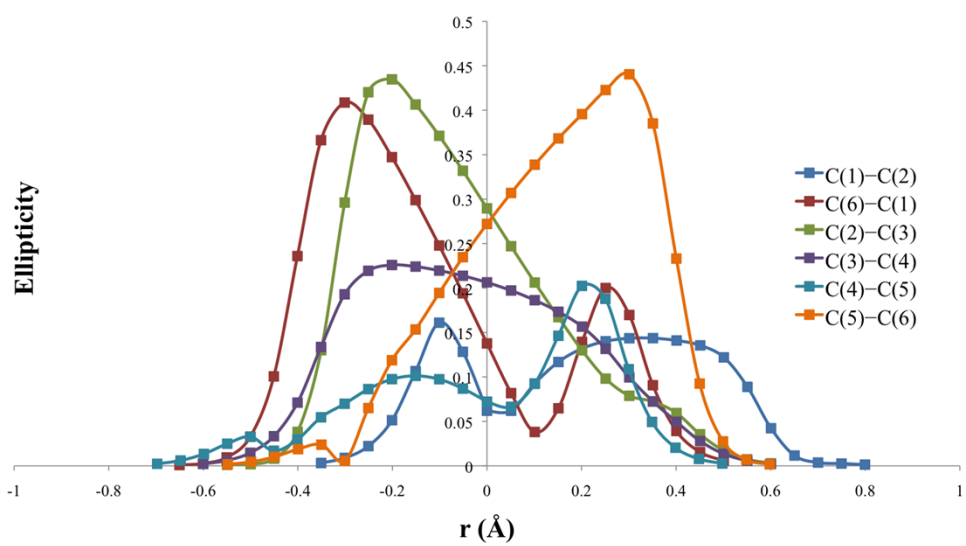


Figure S33: Graph of bond ellipticity along the bond paths for phenyl ring C(1)–C(6) in **8**

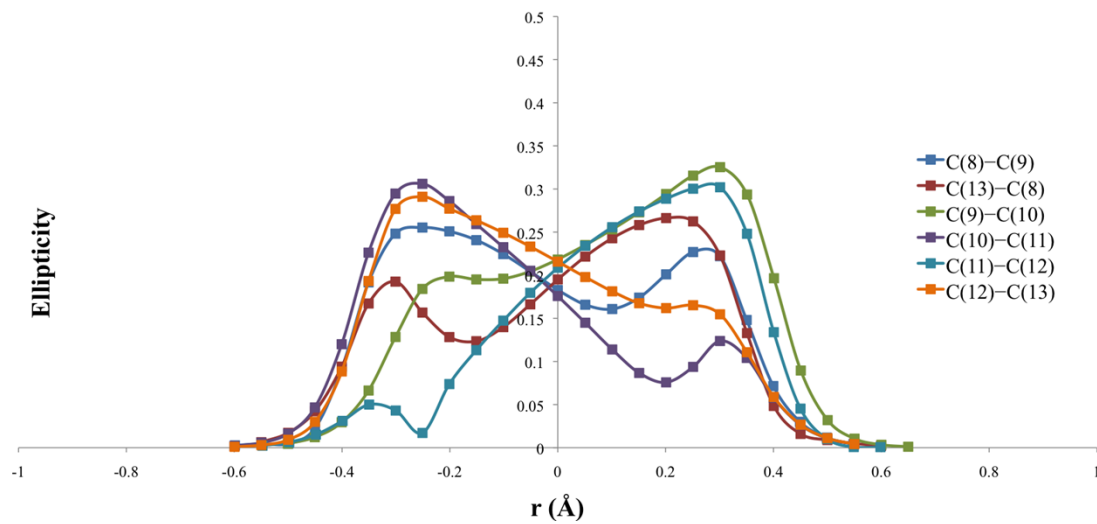


Figure S34: Graph of bond ellipticity along the bond paths for phenyl ring C(8)–C(13) in **8**

c. Bond ellipticity and Laplacian of the electron density profiles for the bonds of the urea moiety in the structures.

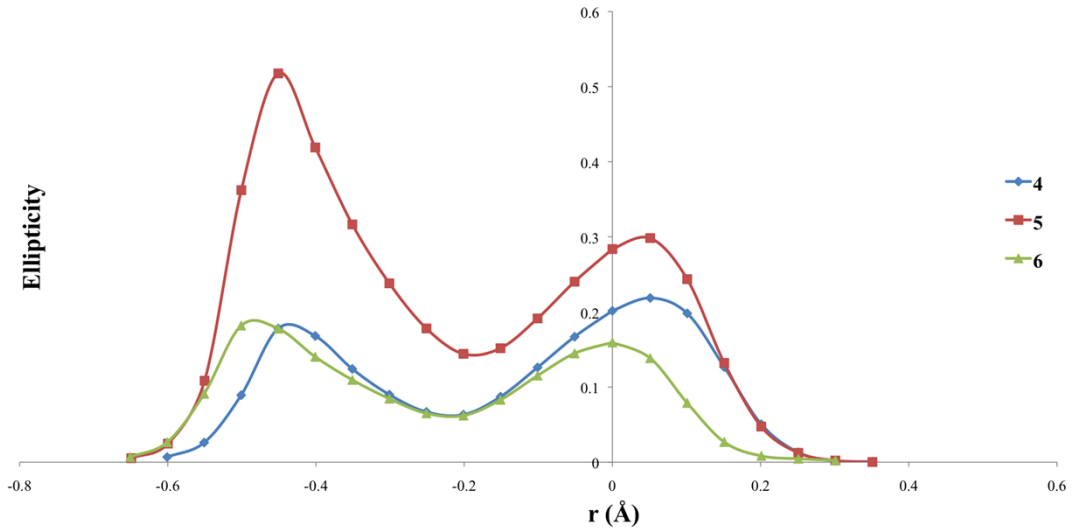


Figure S35: Graph of bond ellipticity along the C(7)-O(1) bond path of the urea group in **4**, **5**, **6**.

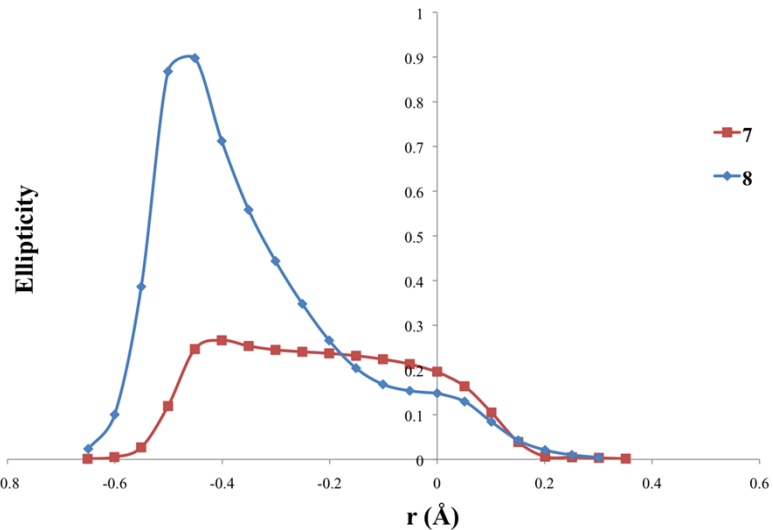


Figure S36: Graph of bond ellipticity along the C(7)-O(1) bond path of the urea group in **7** and **8**.

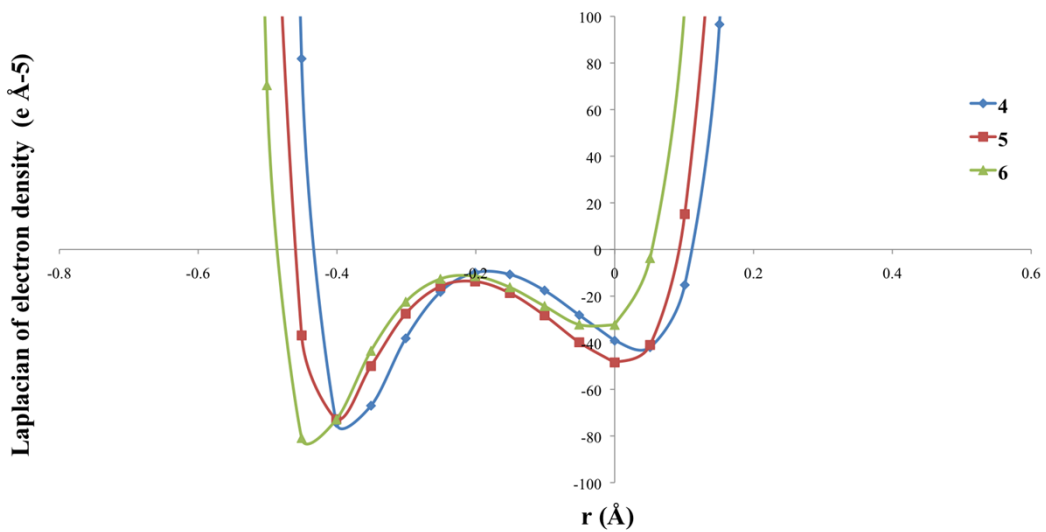


Figure S37: Graph of the $\nabla^2\rho(r)$ along the C(7)-O(1) bond path of the urea group in **4**, **5**, **6**.

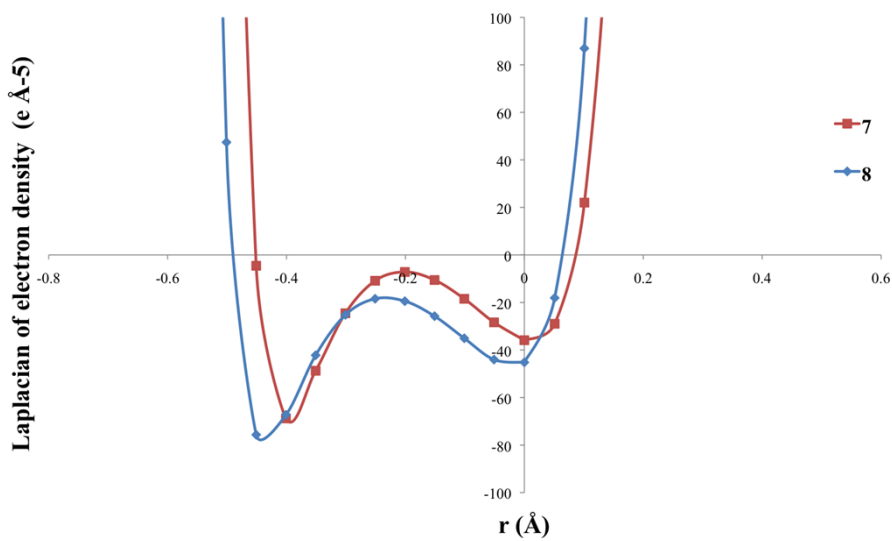


Figure S38: Graph of the $\nabla^2\rho(r)$ along the C(7)-O(1) bond path of the urea group in **7** and **8**.

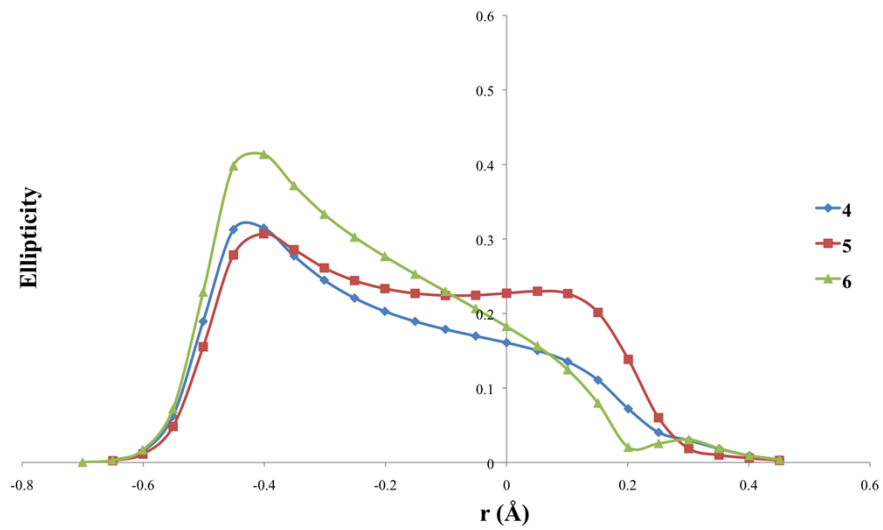


Figure S39: Graph of the bond ellipticity along the N(2)-C(4) bond path of the urea group in **4**, **5**, **6**.

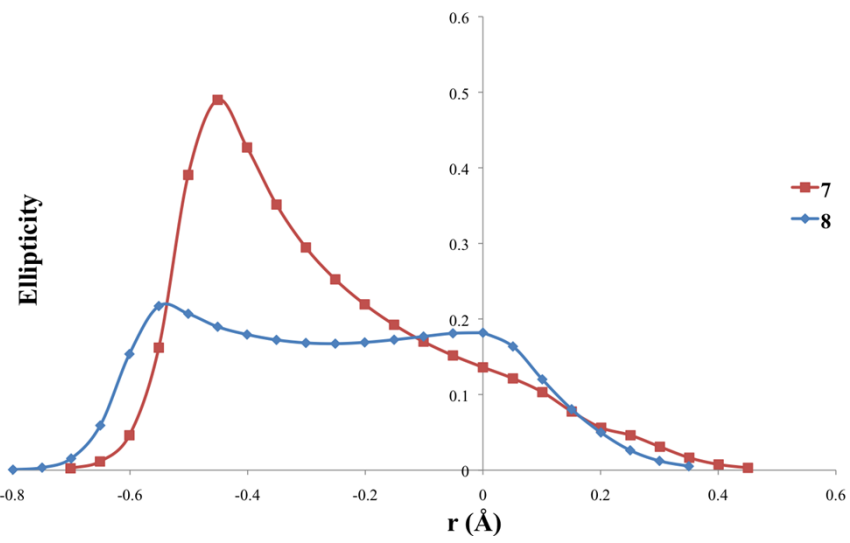


Figure S40: Graph of the bond ellipticity along the N(2)-C(4)/N(3)-C(4) bond path of the urea group in **7** and **8**.

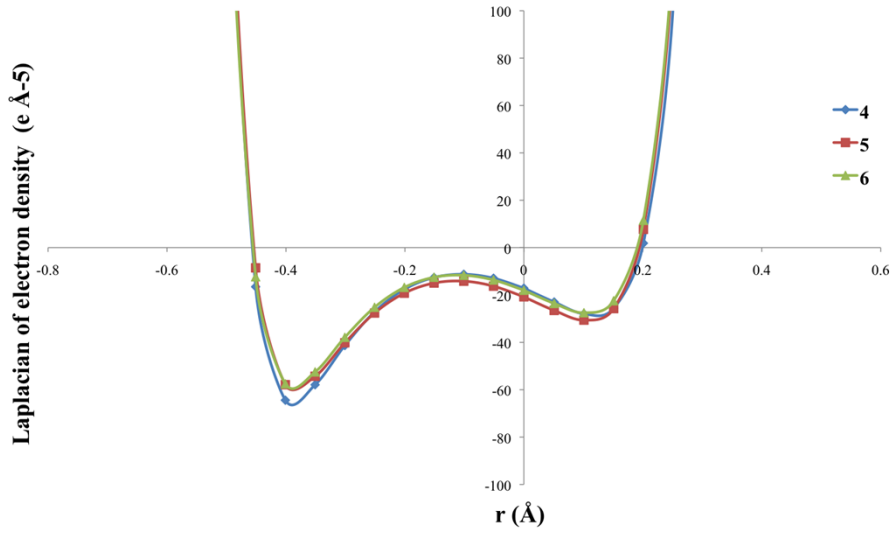


Figure S41: Graph of the $\nabla^2\rho(r)$ along the N(2)-C(4) bond path of the urea group in **4**, **5**, **6**.

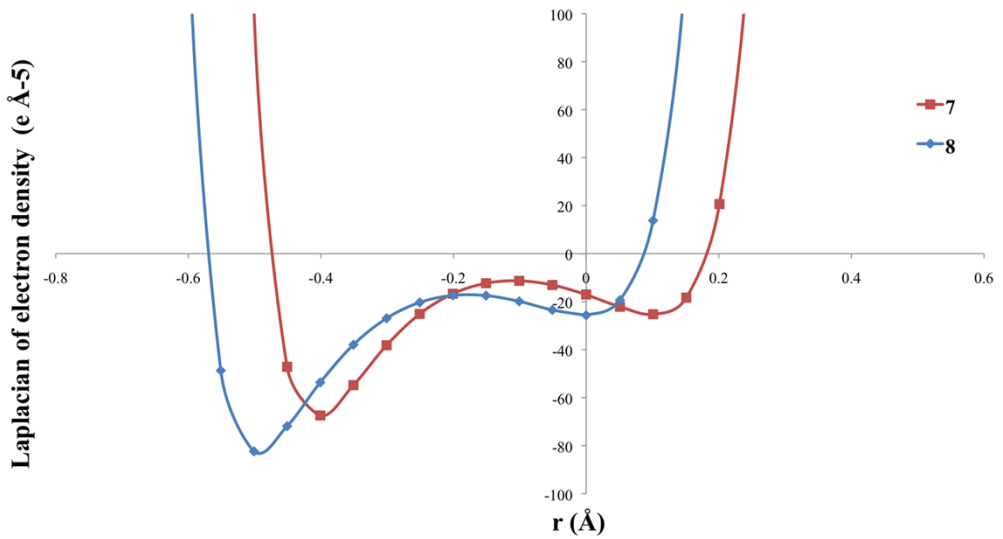


Figure S42: Graph of the $\nabla^2\rho(r)$ along the N(2)-C(4)/ N(3)-C(4) bond path of the urea group in **7** and **8**.

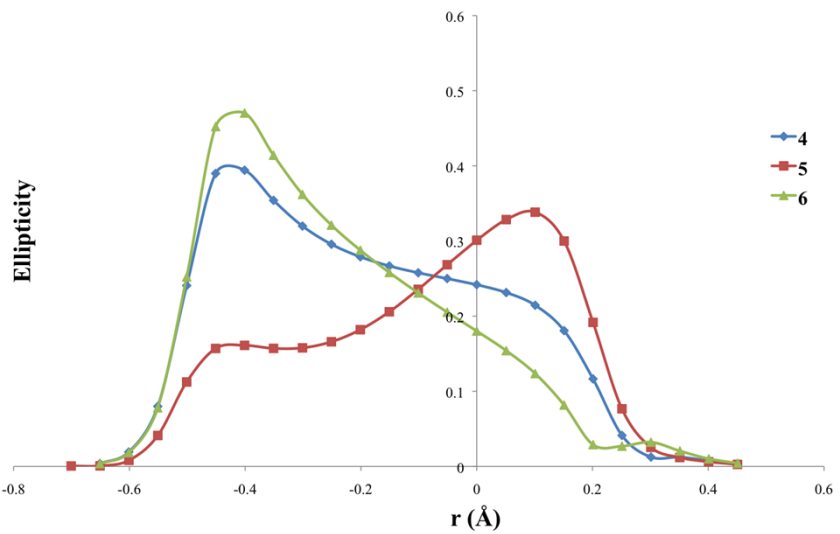


Figure S43: Graph of the bond ellipticity along the N(2)-C(7) bond path of the urea group in **4**, **5**, **6**.

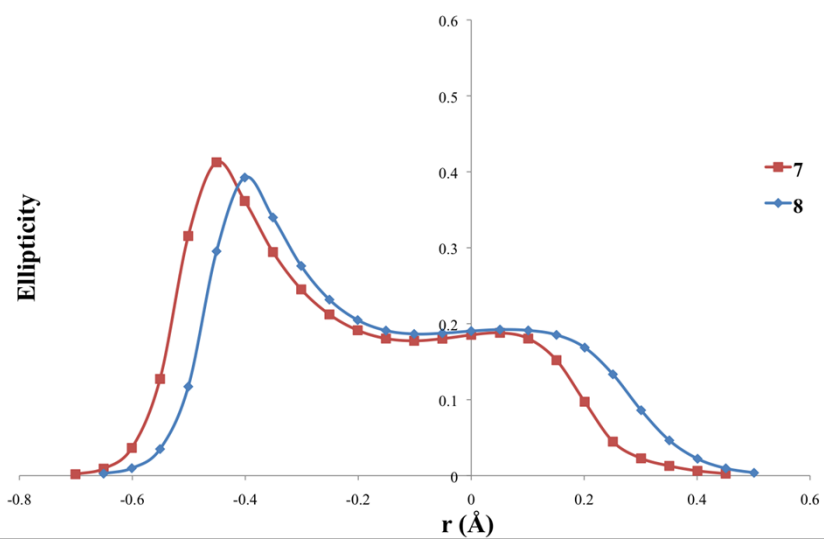


Figure S44: Graph of the bond ellipticity along the N(2)-C(7)/ N(3)-C(7) bond path of the urea group in **7** and **8**.

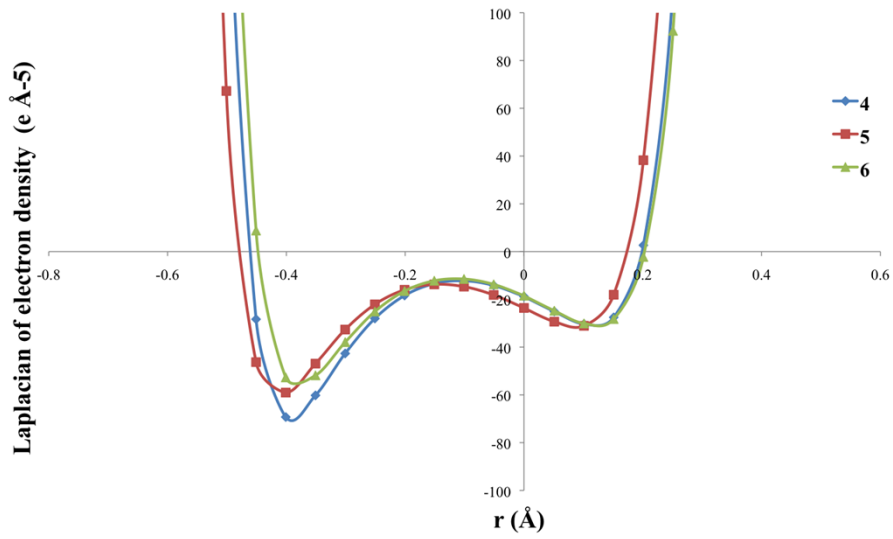


Figure S45: Graph of the $\nabla^2\rho(r)$ along the N(2)-C(7) bond path of the urea group in **4**, **5**, **6**.

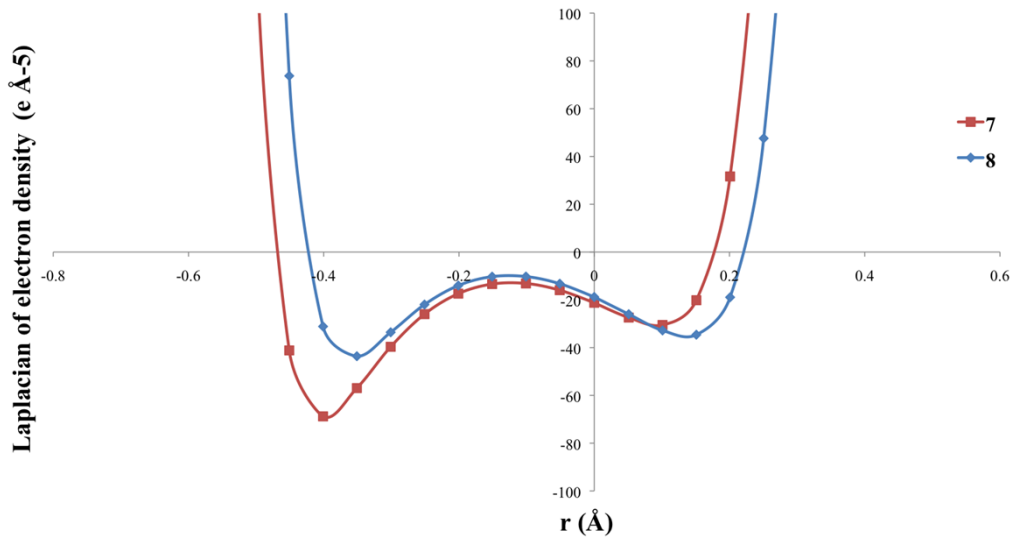


Figure S46: Graph of the $\nabla^2\rho(r)$ along the N(2)-C(7)/N(3)-C(7) bond path of the urea group in **7** and **8**.

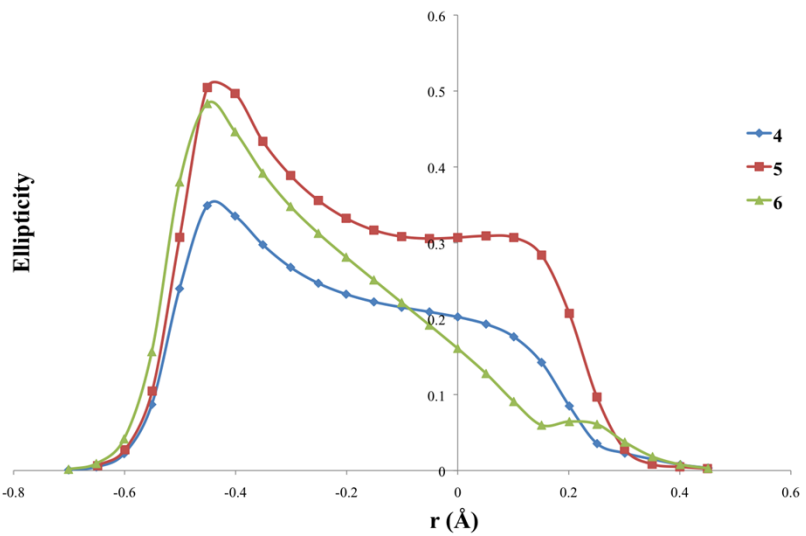


Figure S47: Graph of the bond ellipticity along the N(3)-C(7) bond path of the urea group in **4**, **5**, **6**.

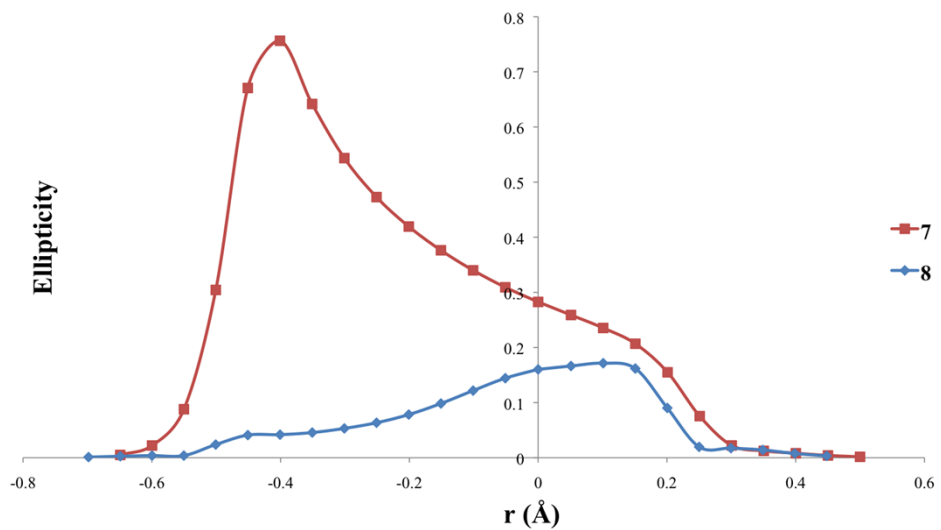


Figure S48: Graph of the bond ellipticity along the N(3)-C(7)/N(4)-C(7) bond path of the urea group in **7** and **8**.

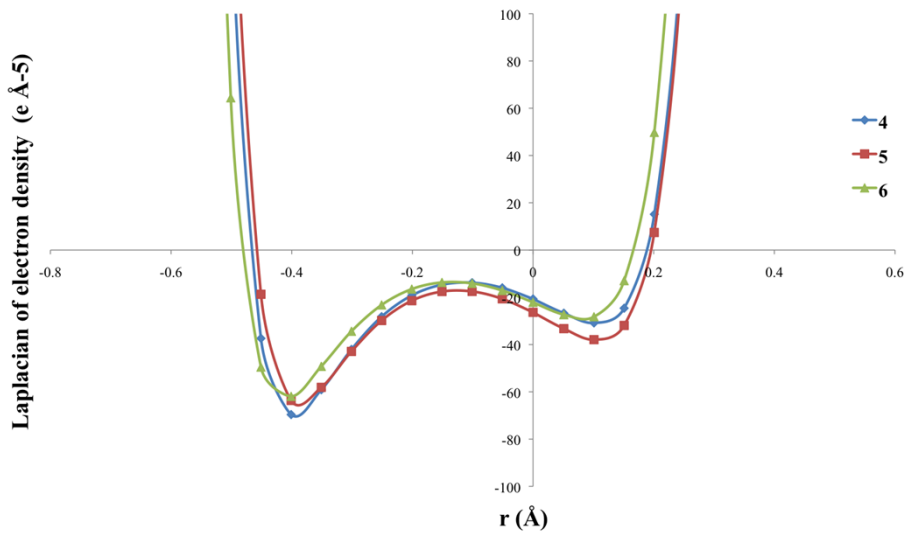


Figure S49: Graph of the $\nabla^2\rho(r)$ along the N(3)-C(7) bond path of the urea group in **4**, **5**, **6**.

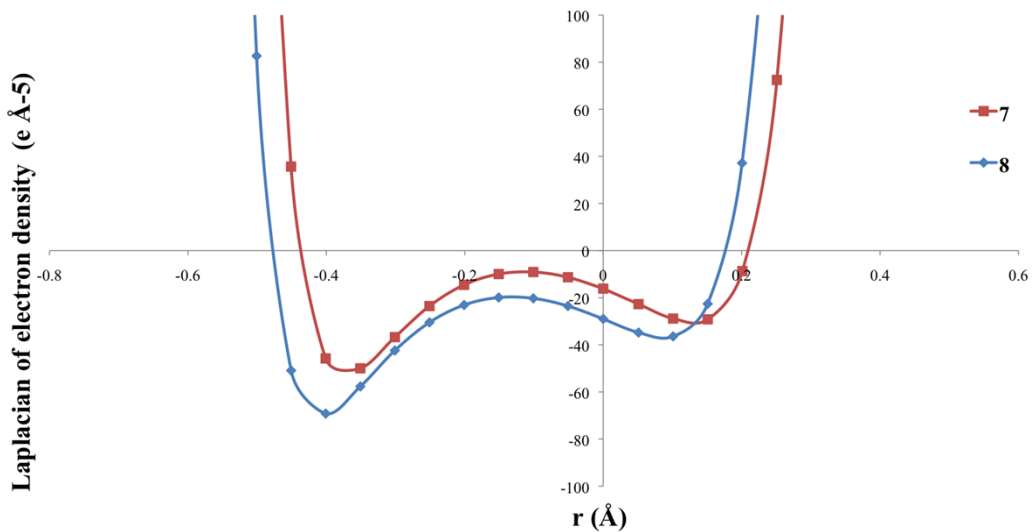


Figure S50: Graph of the $\nabla^2\rho(r)$ along the N(3)-C(7)/ N(4)-C(7) bond path of the urea group in **7** and **8**.

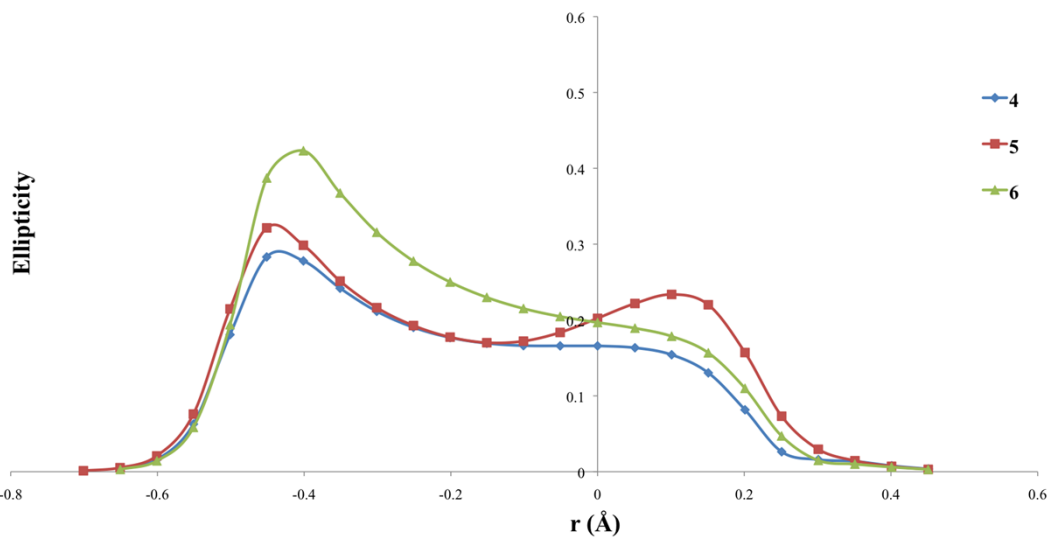


Figure S51: Graph of the bond ellipticity along the N(3)-C(8) bond path of the urea group in **4**, **5**, **6**.

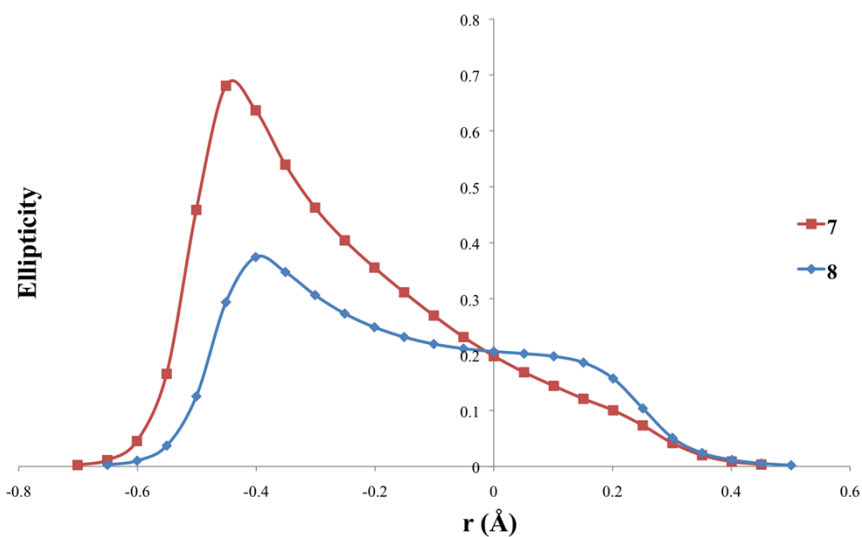


Figure S52: Graph of the bond ellipticity along the N(3)-C(8)/ N(4)-C(8) bond path of the urea group in **7** and **8**.

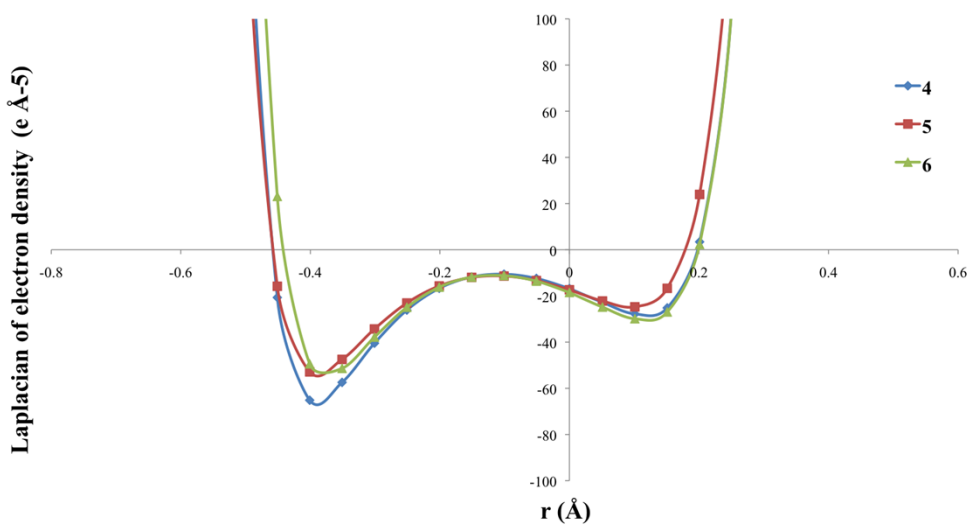


Figure S53: Graph of the $\nabla^2\rho(r)$ along the N(3)-C(8) bond path of the urea group in **4**, **5**, **6**.

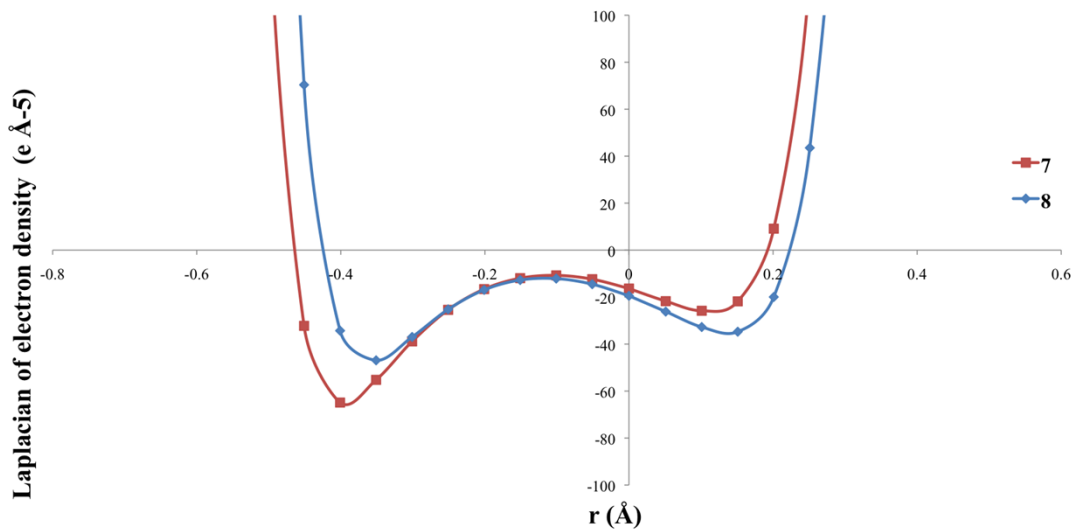


Figure S54: Graph of the $\nabla^2\rho(r)$ along the N(3)-C(8)/N(4)-C(8) bond path of the urea group in **7** and **8**.

4) **QTAIM Charges** of atoms in structures **4 - 8**

a. Table S7: Atomic integrated QTAIM properties ($/e$) of **4**

Atom	Atomic Population (e)	Net charge (e)	Atomic Lagrangian (a.u)
Cl(1)	17.296	-0.296	4.8178 x10 ⁻³
O(1)	9.047	-1.047	1.0811 x10 ⁻⁴
O(2)	8.528	-0.528	2.358 x10 ⁻⁴
O(3)	8.532	-0.532	6.5751 x10 ⁻⁵
O(4)	8.500	-0.500	1.0146 x10 ⁻⁴
O(5)	8.500	-0.500	-1.4803 x10 ⁻⁴
N(1)	6.740	0.260	-1.0396 x10 ⁻³
N(2)	8.098	-1.098	2.8992 x10 ⁻³
N(3)	8.121	-1.121	7.7730 x10 ⁻⁵
N(4)	6.782	0.218	-2.7230 x10 ⁻³
N(5)	7.930	-0.930	1.7449 x10 ⁻²
C(1)	5.823	0.177	1.3921 x10 ⁻³
C(2)	6.096	-0.096	6.2566 x10 ⁻⁴
C(3)	6.111	-0.111	-2.4336 x10 ⁻³
C(4)	5.652	0.348	2.3717 x10 ⁻³
C(5)	6.007	-0.007	2.8160 x10 ⁻³
C(6)	6.049	-0.049	-3.3163 x10 ⁻³
C(7)	4.494	1.506	-4.8031 x10 ⁻³
C(8)	5.660	0.340	5.3388 x10 ⁻³
C(9)	6.114	-0.114	-2.4080 x10 ⁻³
C(10)	6.071	-0.071	4.3161 x10 ⁻³
C(11)	5.787	0.213	5.5666 x10 ⁻³
C(12)	5.979	0.021	2.7422 x10 ⁻³
C(13)	6.008	-0.008	3.1211 x10 ⁻³
C(14)	5.826	0.174	-7.4033 x10 ⁻³
C(15)	5.782	0.218	-6.5715 x10 ⁻³
C(16)	5.851	0.149	-2.8639 x10 ⁻³
C(17)	5.806	0.194	-6.0781 x10 ⁻³
H(2)	0.846	0.154	1.3955 x10 ⁻⁴
H(3)	0.819	0.181	-9.6069 x10 ⁻⁶
H(5)	0.766	0.234	1.0429 x10 ⁻⁴
H(6)	0.817	0.183	8.8546 x10 ⁻⁵
H(9)	0.749	0.251	-2.9003 x10 ⁻⁵
H(10)	0.803	0.197	-8.5883 x10 ⁻⁵
H(12)	0.844	0.156	-3.7284 x10 ⁻⁴
H(13)	0.794	0.206	3.3874 x10 ⁻⁴
H(14A)	0.949	0.051	-1.0725 x10 ⁻⁵
H(14B)	0.952	0.048	1.4915 x10 ⁻⁴

H(14C)	0.881	0.119	-1.3456 x10 ⁻⁵
H(15A)	0.950	0.050	-2.5833 x10 ⁻⁵
H(15B)	0.940	0.060	-1.2954 x10 ⁻⁴
H(15C)	0.976	0.024	1.5374 x10 ⁻⁴
H(16A)	0.966	0.034	6.0685 x10 ⁻⁵
H(16B)	0.932	0.068	6.8646 x10 ⁻⁵
H(16C)	0.908	0.092	5.9650 x10 ⁻⁵
H(17A)	0.906	0.093	1.2846 x10 ⁻⁴
H(17B)	0.974	0.026	7.4247 x10 ⁻⁵
H(17C)	0.929	0.071	7.6634 x10 ⁻⁵
H(2A)	0.566	0.434	-4.7707 x10 ⁻⁵
H(3A)	0.539	0.461	4.3218 x10 ⁻⁴

b. Table S8: Atomic integrated QTAIM properties ($/e$) of **5**

Atom	Atomic Population (e)	Net charge (e)	Atomic Lagrangian (a.u)
O(1)	9.052	-1.052	2.9712 x10 ⁻⁴
O(2)	8.358	-0.358	5.0352 x10 ⁻⁴
O(3)	8.359	-0.359	6.2221 x10 ⁻⁵
O(4)	8.409	-0.409	-7.9510 x10 ⁻⁶
O(5)	8.418	-0.412	-7.4437 x10 ⁻⁶
O(6)	9.103	-1.103	2.5813 x10 ⁻⁴
O(7)	9.113	-1.133	7.8101 x10 ⁻⁴
N(1)	6.983	0.017	2.1194 x10 ⁻⁴
N(2)	8.165	-1.165	3.9730 x10 ⁻⁴
N(3)	8.070	-1.070	2.9803 x10 ⁻³
N(4)	6.858	0.142	-2.5592 x10 ⁻⁴
N(5)	7.905	-0.905	-2.4760 x10 ⁻³
C(1)	5.738	0.262	3.7768 x10 ⁻⁴
C(2)	6.175	-0.175	9.1148 x10 ⁻⁴
C(3)	6.194	-0.194	3.8941 x10 ⁻³
C(4)	5.685	0.315	2.3618 x10 ⁻³
C(5)	6.145	-0.145	2.1528 x10 ⁻³
C(6)	6.094	-0.094	3.3924 x10 ⁻³
C(7)	4.309	1.691	-6.9819 x10 ⁻³
C(8)	5.673	0.327	-1.2197 x10 ⁻²
C(9)	6.200	-0.200	2.1128 x10 ⁻⁴
C(10)	5.852	0.148	2.4140 x10 ⁻³
C(11)	5.804	0.196	-4.4653 x10 ⁻³
C(12)	6.097	-0.096	1.1573 x10 ⁻³
C(13)	6.006	-0.006	5.6591 x10 ⁻⁴
C(14)	6.074	-0.074	1.2094 x10 ⁻²
C(15)	5.878	0.122	9.4041 x10 ⁻³
C(16)	5.923	0.077	8.7482 x10 ⁻³
C(17)	5.939	0.061	1.0953 x10 ⁻²
C(18)	4.515	1.485	8.6268 x10 ⁻⁶

C(19)	6.251	-0.251	8.2879 x10 ⁻³
H(2)	0.862	0.138	-79712 x10 ⁻⁶
H(3)	0.826	0.174	3.2353 x10 ⁻⁴
H(5)	0.820	0.180	5.6993 x10 ⁻⁵
H(6)	0.688	0.312	1.1316 x10 ⁻⁴
H(9)	0.789	0.211	1.6491 x10 ⁻⁴
H(10)	0.836	0.164	-7.8876 x10 ⁻⁵
H(12)	0.831	0.169	2.6326 x10 ⁻⁵
H(13)	0.796	0.204	1.3524 x10 ⁻⁴
H(14A)	0.803	0.197	4.6932 x10 ⁻⁵
H(14B)	0.792	0.208	-1.0501 x10 ⁻⁵
H(14C)	0.812	0.188	4.0416 x10 ⁻⁶
H(15A)	0.809	0.191	-9.2525 x10 ⁻⁵
H(15B)	0.961	0.039	-6.0710 x10 ⁻⁵
H(15C)	0.939	0.061	4.3633 x10 ⁻⁵
H(16A)	0.983	0.017	2.1774 x10 ⁻⁴
H(16B)	0.775	0.225	1.9768 x10 ⁻⁵
H(16C)	0.930	0.070	1.1156 x10 ⁻⁵
H(17A)	0.994	0.006	2.9108 x10 ⁻⁴
H(17B)	0.882	0.118	2.8101 x10 ⁻⁴
H(17C)	0.847	0.153	7.0459 x10 ⁻⁴
H(19A)	0.926	0.074	2.8138 x10 ⁻⁵
H(19B)	0.829	0.171	1.0211 x10 ⁻⁵
H(19C)	0.918	0.082	-2.1897 x10 ⁻⁵
H(2A)	0.443	0.557	-7.2685 x10 ⁻⁴
H(3A)	0.519	0.481	2.5838 x10 ⁻⁴

c. Table S9: Atomic integrated QTAIM properties ($/e$) of **6**

Atom	Atomic Population (e)	Net charge (e)	Atomic Lagrangian (a.u)
F(1)	9.290	-0.290	-5.7809 x10 ⁻⁴
O(1)	9.011	-1.011	-1.2643 x10 ⁻⁴
O(2)	8.324	-0.324	-2.6075 x10 ⁻⁵
O(3)	8.318	-0.318	4.6422 x10 ⁻⁴
O(4)	8.351	-0.351	2.6827 x10 ⁻⁴
O(5)	8.350	-0.350	-2.2867 x10 ⁻⁵
N(1)	6.897	0.103	6.4623 x10 ⁻³
N(2)	7.970	-0.970	7.7008 x10 ⁻⁴
N(3)	8.062	-1.062	-3.2674 x10 ⁻³
N(4)	6.875	0.125	-2.5049 x10 ⁻³
N(5)	7.917	-0.917	-4.5423 x10 ⁻³
C(1)	5.701	0.299	-1.5430 x10 ⁻³
C(2)	6.147	-0.147	1.0896 x10 ⁻³
C(3)	5.967	0.033	3.6940 x10 ⁻³
C(4)	5.756	0.244	3.0926 x10 ⁻³

C(5)	6.081	-0.081	2.3509 x10 ⁻³
C(6)	6.079	-0.079	1.9248 x10 ⁻³
C(7)	4.399	1.601	-1.3263 x10 ⁻²
C(8)	5.633	0.367	-1.1486 x10 ⁻²
C(9)	6.105	-0.105	-7.7499 x10 ⁻⁴
C(10)	6.107	-0.107	-7.4777 x10 ⁻³
C(11)	5.788	0.212	-7.9231 x10 ⁻³
C(12)	6.109	-0.109	7.1514 x10 ⁻⁴
C(13)	5.920	0.080	-4.5570 x10 ⁻³
C(14A)	5.716	0.284	8.2182 x10 ⁻³
C(15A)	5.724	0.276	1.6918 x10 ⁻³
C(14B)	5.726	0.274	-2.0186 x10 ⁻³
C(15B)	5.708	0.292	1.5590 x10 ⁻²
H(2)	0.796	0.204	-9.3670 x10 ⁻⁵
H(3)	0.846	0.154	7.1222 x10 ⁻⁶
H(5)	0.838	0.162	1.3013 x10 ⁻⁴
H(6)	0.869	0.131	3.2640 x10 ⁻⁵
H(9)	0.902	0.098	-2.5723 x10 ⁻⁶
H(10)	0.877	0.123	9.7757 x10 ⁻⁵
H(12)	0.863	0.137	-7.1401 x10 ⁻⁵
H(13)	0.825	0.175	-1.6582 x10 ⁻³
H(14A)	1.015	-0.015	-2.2952 x10 ⁻⁵
H(14B)	1.016	-0.016	-6.9204 x10 ⁻⁵
H(14C)	1.016	-0.016	-1.1389 x10 ⁻⁴
H(15A)	1.015	-0.015	-5.4371 x10 ⁻⁵
H(15B)	1.015	-0.015	-6.3879 x10 ⁻⁶
H(15C)	1.015	-0.015	2.2826 x10 ⁻⁵
H(14D)	1.016	-0.016	-5.9992 x10 ⁻⁵
H(14E)	1.015	-0.015	2.3673 x10 ⁻⁵
H(14F)	1.018	-0.018	-5.2172 x10 ⁻⁴
H(15D)	1.016	-0.016	-2.0492 x10 ⁻⁵
H(15E)	1.015	-0.015	8.1611 x10 ⁻⁵
H(15F)	1.015	-0.015	-8.1807 x10 ⁻⁵
H(2A)	0.549	0.451	7.8159 x10 ⁻⁴
H(3A)	0.565	0.435	1.8583 x10 ⁻³

d. Table S10: Atomic integrated QTAIM properties ($/e$) of 7

Atom	Atomic Population (e)	Net charge (e)	Atomic Lagrangian (a.u)
Cl(1)	17.482	-0.482	5.1171 x10 ⁻³
O(1)	8.890	-0.890	4.621 x10 ⁻⁴
O(2)	8.370	-0.370	-3.9625 x10 ⁻⁵
O(3)	8.373	-0.373	2.4369 x10 ⁻⁵
O(4)	8.385	-0.385	1.7030 x10 ⁻⁵
O(5)	8.376	-0.376	-1.9000 x10 ⁻⁵
N(1)	6.717	0.283	-5.3033 x10 ⁻⁵

N(2)	8.159	-1.159	4.2163 x10 ⁻³
N(3)	8.014	-1.014	-3.7288 x10 ⁻⁴
N(4)	6.731	0.269	-6.2319 x10 ⁻³
N(5)	7.812	-0.812	-5.3608 x10 ⁻³
C(1)	6.136	-0.136	1.6192 x10 ⁻³
C(2)	6.051	-0.051	2.3200 x10 ⁻³
C(3)	6.188	-0.188	-1.9964 x10 ⁻³
C(4)	5.564	0.436	4.4844 x10 ⁻³
C(5)	6.099	-0.099	1.5926 x10 ⁻³
C(6)	5.708	0.292	5.8421 x10 ⁻⁴
C(7)	4.497	1.503	-5.6654 x10 ⁻⁴
C(8)	5.627	0.373	-3.8448 x10 ⁻³
C(9)	6.050	-0.050	-1.2366 x10 ⁻³
C(10)	5.936	0.064	2.1686 x10 ⁻³
C(11)	6.069	-0.069	1.3039 x10 ⁻⁴
C(12)	5.771	0.229	1.2607 x10 ⁻³
C(13)	6.060	-0.060	2.5721 x10 ⁻³
C(14)	6.168	-0.168	5.3022 x10 ⁻³
C(15)	6.027	-0.027	5.1650 x10 ⁻³
C(16)	5.963	0.037	1.0397 x10 ⁻²
C(17)	6.025	-0.025	6.1925 x10 ⁻³
H(1)	0.874	0.126	2.1925 x10 ⁻⁴
H(2)	0.997	0.003	-5.4225 x10 ⁻⁶
H(3)	0.838	0.162	1.3715 x10 ⁻⁵
H(5)	0.769	0.231	7.1964 x10 ⁻⁴
H(9)	0.893	0.107	4.9589 x10 ⁻⁵
H(10)	0.908	0.092	-2.1992 x10 ⁻⁵
H(11)	0.881	0.119	-1.9698 x10 ⁻⁵
H(13)	0.766	0.234	4.6134 x10 ⁻⁴
H(14A)	0.899	0.101	3.3242 x10 ⁻⁴
H(14B)	0.756	0.244	4.3147 x10 ⁻⁵
H(14C)	0.839	0.161	2.6713 x10 ⁻⁵
H(15A)	0.847	0.153	3.3593 x10 ⁻⁴
H(15B)	0.965	0.035	6.9625 x10 ⁻⁴
H(15C)	0.884	0.116	-4.7933 x10 ⁻⁴
H(16A)	0.940	0.060	5.0646 x10 ⁻⁵
H(16B)	0.862	0.138	2.0053 x10 ⁻⁵
H(16C)	0.918	0.082	-3.7317 x10 ⁻⁴
H(17A)	0.836	0.164	-2.8347 x10 ⁻⁵
H(17B)	1.055	-0.055	-7.4447 x10 ⁻⁵
H(17C)	0.872	0.128	-2.8063 x10 ⁻⁴
H(2A)	0.485	0.515	2.3498 x10 ⁻⁴
H(3A)	0.561	0.439	-6.6159 x10 ⁻⁴

e. Table S11: Atomic integrated QTAIM properties ($/e$) of **8**

Atom	Atomic Population (e)	Net charge (e)	Atomic Lagrangian (a.u)
O(1)	8.846	-0.846	-7.0875 x 10 ⁻⁴
O(2)	8.278	-0.278	1.5247 x 10 ⁻⁴
O(3)	8.291	-0.291	-4.9568 x 10 ⁻⁶
O(4)	8.251	-0.251	2.3551 x 10 ⁻⁵
O(5)	8.246	-0.246	-8.5715 x 10 ⁻⁶
O(6)	8.268	-0.268	5.0366 x 10 ⁻⁵
O(7)	8.277	-0.277	4.6423 x 10 ⁻⁴
O(8)	8.297	-0.297	1.3943 x 10 ⁻⁵
O(9)	8.298	-0.298	4.6710 x 10 ⁻⁵
O(10)	8.992	-0.992	2.0531 x 10 ⁻⁴
O(11)	9.217	-1.217	-3.5004 x 10 ⁻⁴
N(1)	6.773	0.227	-1.2743 x 10 ⁻²
N(2)	6.873	0.127	6.1789 x 10 ⁻³
N(3)	8.047	-1.047	-1.3347 x 10 ⁻³
N(4)	7.916	-0.916	3.4216 x 10 ⁻⁴
N(5)	6.884	0.116	7.3208 x 10 ⁻³
N(6)	6.734	0.266	-8.6235 x 10 ⁻⁵
N(7)	8.006	-1.006	6.5106 x 10 ⁻⁴
C(1)	5.683	0.317	-1.2325 x 10 ⁻³
C(2)	6.093	-0.093	1.5860 x 10 ⁻⁴
C(3)	6.234	-0.234	4.8258 x 10 ⁻³
C(4)	5.610	0.390	4.8528 x 10 ⁻³
C(5)	5.872	0.128	2.8971 x 10 ⁻³
C(6)	5.920	0.080	1.3555 x 10 ⁻³
C(7)	4.281	1.719	2.9280 x 10 ⁻³
C(8)	5.642	0.358	-8.9396 x 10 ⁻³
C(9)	5.890	0.110	-1.5112 x 10 ⁻³
C(10)	5.893	0.107	-1.1379 x 10 ⁻³
C(11)	5.871	0.129	-1.7484 x 10 ⁻³
C(12)	5.832	0.168	-3.3819 x 10 ⁻⁴
C(13)	6.073	-0.073	3.6108 x 10 ⁻³
C(14)	5.825	0.175	6.9427 x 10 ⁻³
C(15)	5.702	0.298	-8.6048 x 10 ⁻³
C(16)	5.872	0.128	9.7070 x 10 ⁻³
C(17)	5.648	0.352	2.1165 x 10 ⁻³
C(18)	4.534	1.466	3.1791 x 10 ⁻²
C(19)	6.720	-0.720	-3.0814 x 10 ⁻³
H(1)	0.848	0.152	7.3486 x 10 ⁻⁵
H(3)	0.870	0.130	1.1534 x 10 ⁻⁵
H(5)	0.768	0.232	2.0058 x 10 ⁻⁴
H(9)	0.902	0.098	2.3216 x 10 ⁻⁴
H(11)	0.929	0.071	-8.2577 x 10 ⁻⁵
H(13)	0.985	0.015	-8.1822 x 10 ⁻⁴
H(14A)	0.916	0.084	2.7576 x 10 ⁻⁵

H(14B)	0.921	0.079	1.9301×10^{-5}
H(14C)	0.989	0.011	1.3764×10^{-5}
H(15A)	0.944	0.056	-2.1637×10^{-5}
H(15B)	0.746	0.254	-2.1455×10^{-5}
H(15C)	0.954	0.046	-8.1557×10^{-4}
H(16A)	0.937	0.063	4.9775×10^{-5}
H(16B)	0.899	0.101	2.4337×10^{-4}
H(16C)	0.978	0.022	-6.9631×10^{-5}
H(17A)	0.941	0.059	7.2743×10^{-5}
H(17B)	1.003	-0.003	-2.7784×10^{-4}
H(17C)	0.975	0.025	-5.3444×10^{-7}
H(19A)	0.489	0.511	-1.9586×10^{-7}
H(19B)	0.720	0.280	-3.1018×10^{-6}
H(19C)	0.625	0.375	-6.5990×10^{-5}
H(3A)	0.679	0.321	-1.0152×10^{-3}
H(4A)	0.590	0.410	5.9298×10^{-5}

5) Proton NMR titration studies

a. Methodology

Proton NMR titration experiments of the receptors with the acetate, chloride and fluoride anions were performed to investigate the dynamics of the solution state binding of the receptors. The tetramethylammonium acetate salt was used however due to difficulties in the solubility of the tetramethylammonium chloride and fluoride salts in the 0.5% d₆-DMSO-H₂O solvent system, in these cases the tetrabutylammonium halide salts were used. Titrations with tetrabutylammonium hydroxide with receptors **1** and **3** were conducted to characterise the deprotonation of these receptors in solution.

Proton NMR (300 MHz) were determined on a Bruker AV300 spectrometer with chemical shifts reported in parts per million (ppm), calibrated to the solvent peak.

1.5 mL of a 0.01 M solution of the receptor was prepared. Of this solution, 0.5 mL was added to an NMR tube, which was then sealed with an air tight suba seal. The remaining 1 mL of the receptor solution was used to make a 0.15 M solution of the desired guest. The anion/receptor solution was titrated into the NMR tube in small aliquots and a ¹H NMR spectrum was recorded after each addition. This resulted in an increasing concentration of guest throughout the experiment while the receptor concentration was kept constant.

The binding constants were obtained using the WinEQNMR¹¹ software.

b. Stack Plot and Fit Plot for receptor **1** with TMA acetate

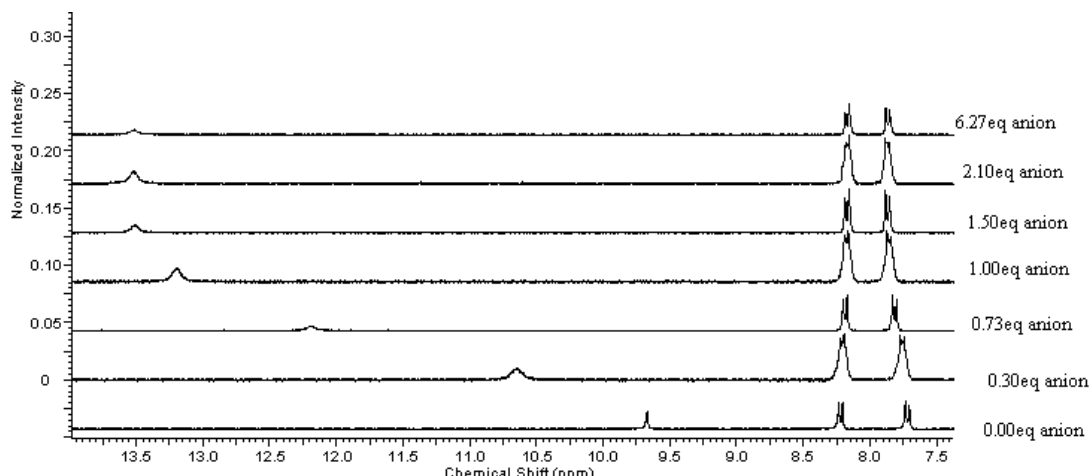


Figure S55: Stack Plot of titration of receptor **1** with TMA acetate

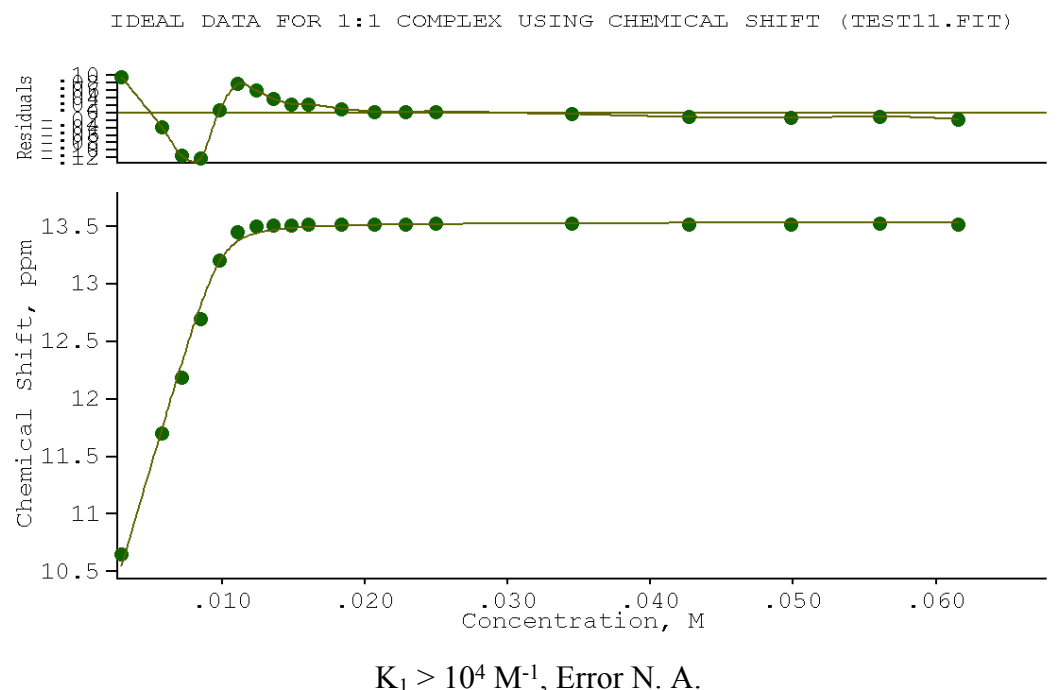


Figure S56: Fit Plot of titration of receptor **1** with TMA acetate

c. Stack Plot and Fit Plot for receptor **1** with TBA chloride

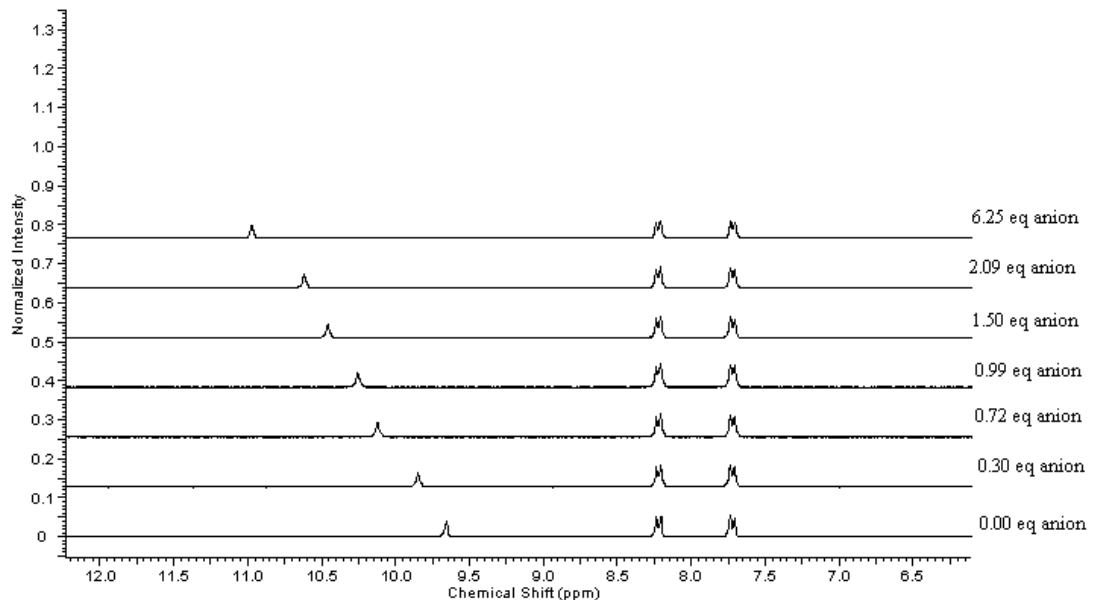


Figure S57: Stack Plot of titration of receptor **1** with TBA chloride

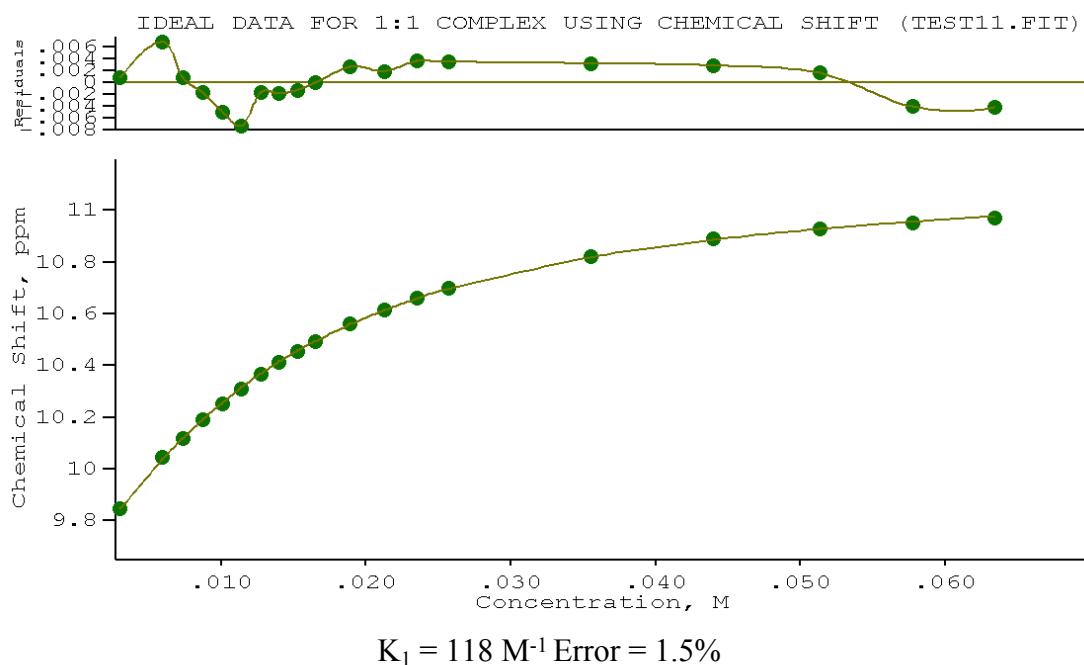


Figure S58: Fit Plot of titration of receptor **1** with TBA chloride

d. Stack Plot for receptor **1** with TBA fluoride

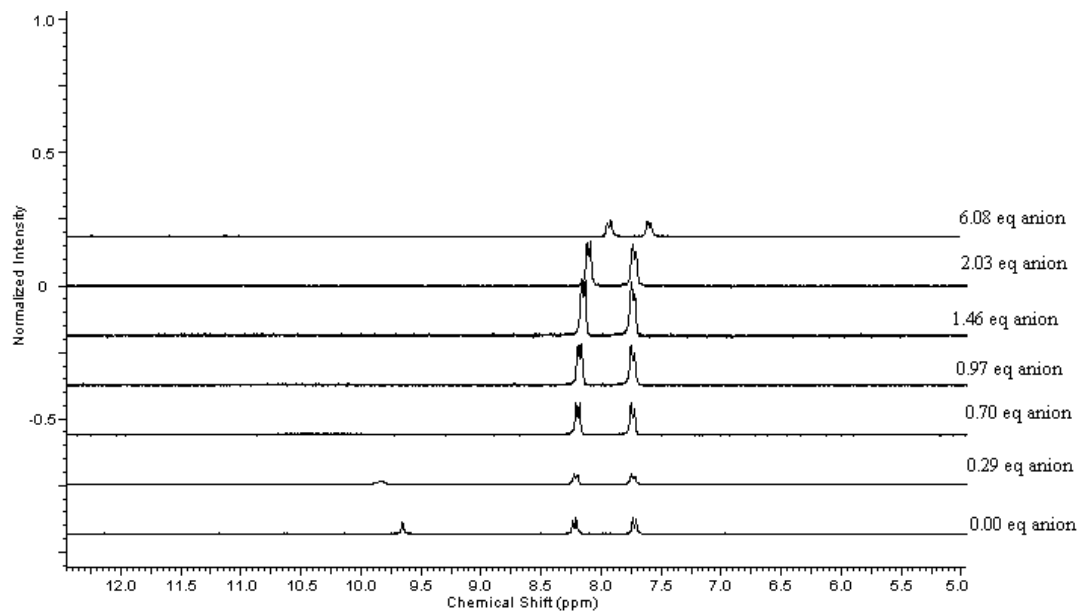


Figure S59: Stack Plot of titration of receptor **1** with TBA fluoride

e. Stack Plot for receptor **1** with TBA hydroxide

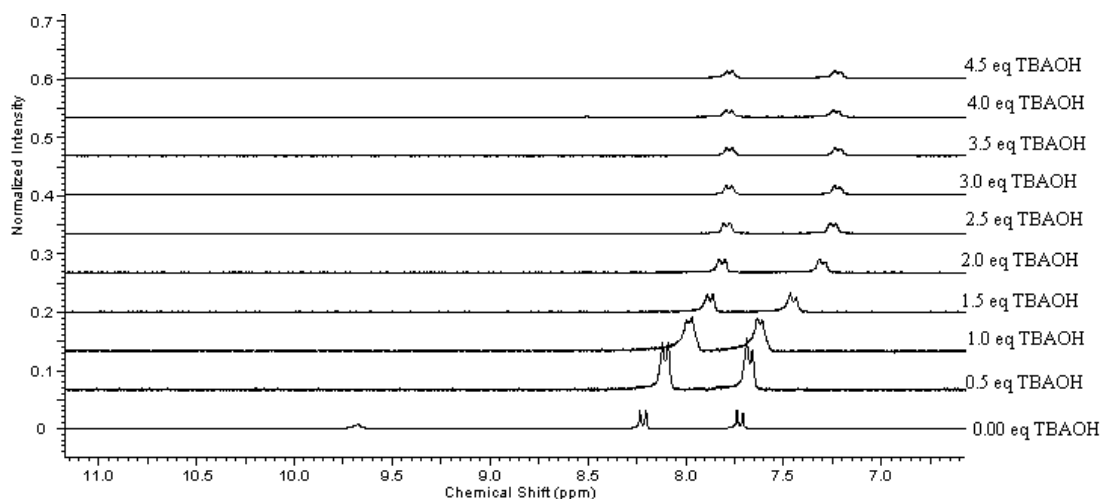


Figure S60: Stack Plot of titration of receptor **1** with TBA hydroxide

f. Stack Plot of receptor **2** with TBA chloride

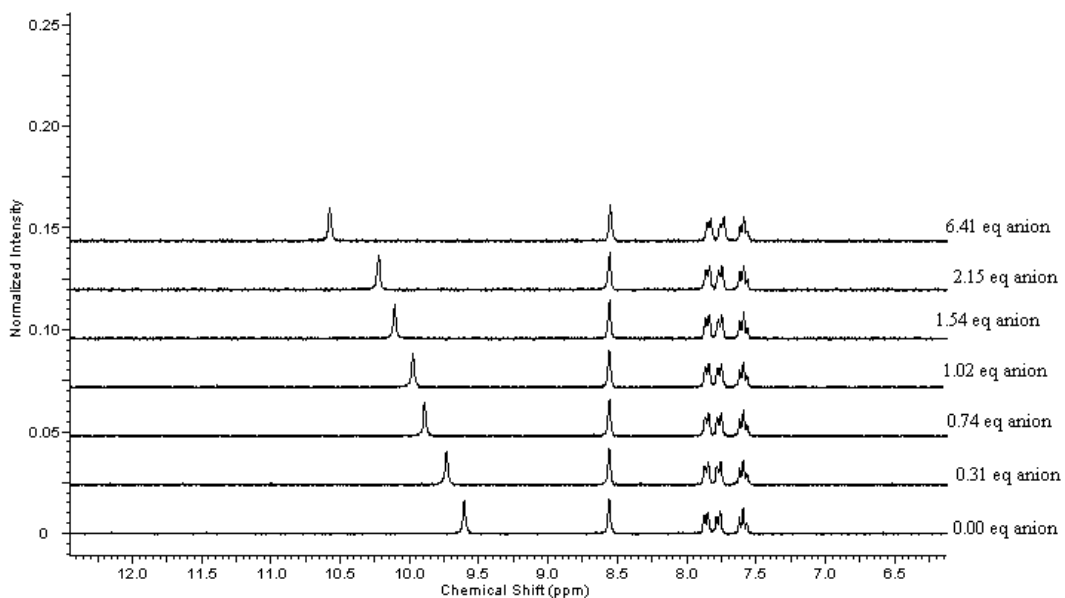


Figure S61: Stack Plot of titration of receptor **2** with TBA chloride

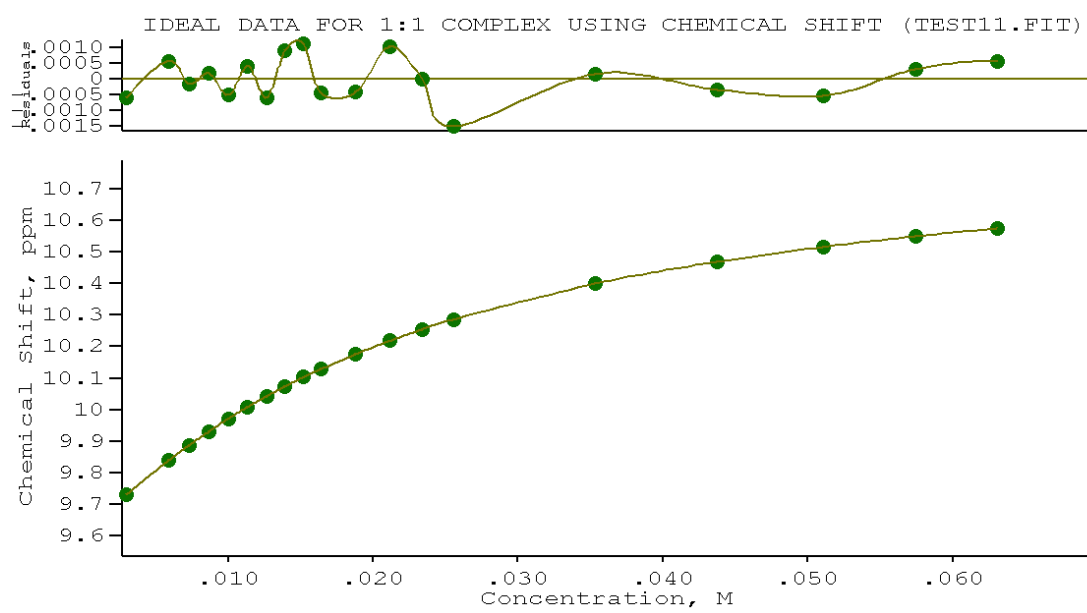


Figure S62: Fit Plot of titration of receptor **2** with TBA chloride

g. Stack Plot and Fit Plot of receptor **3** with TMA acetate

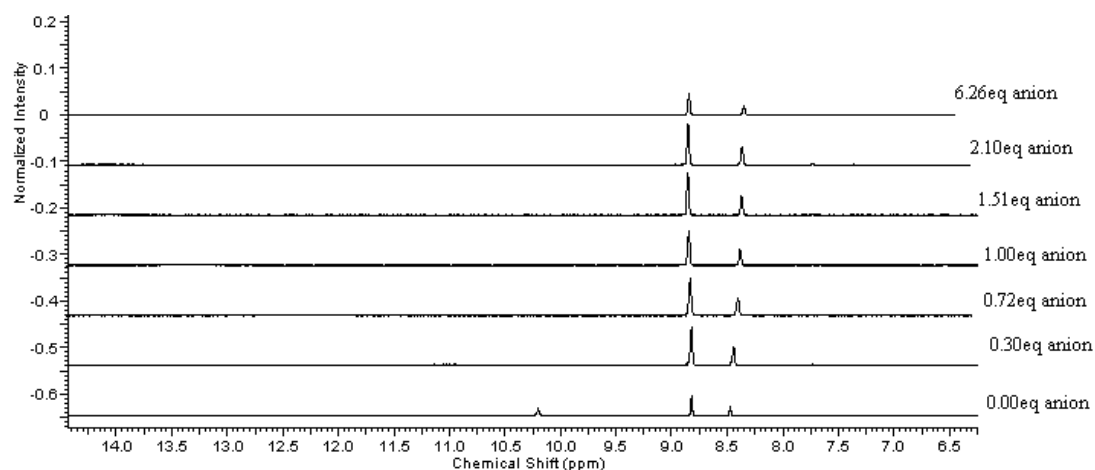


Figure S63: Stack Plot of titration of receptor **3** with TMA acetate

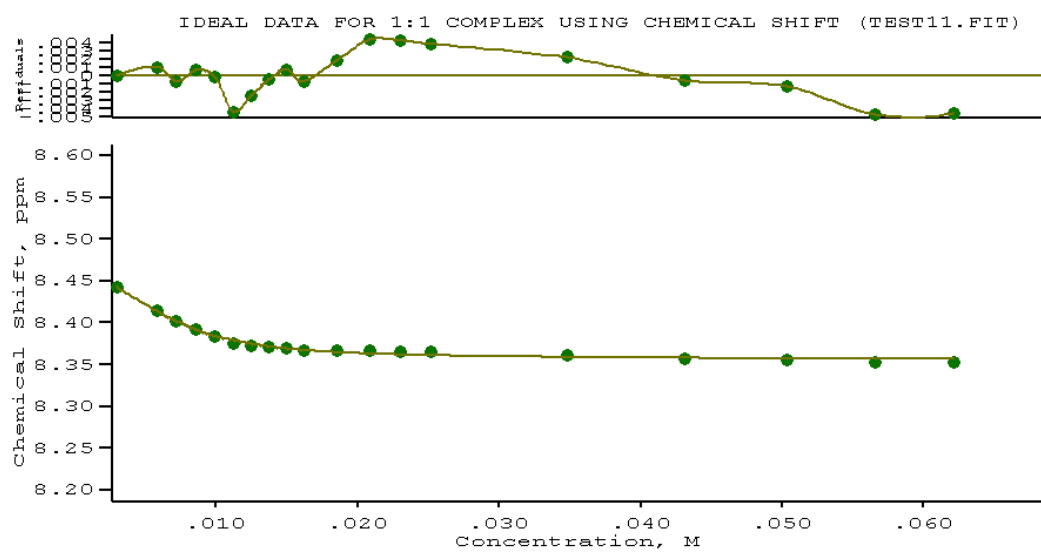


Figure S64: Fit Plot of titration of receptor **2** with TMA acetate

h. Stack Plot for receptor **3** with TBA hydroxide

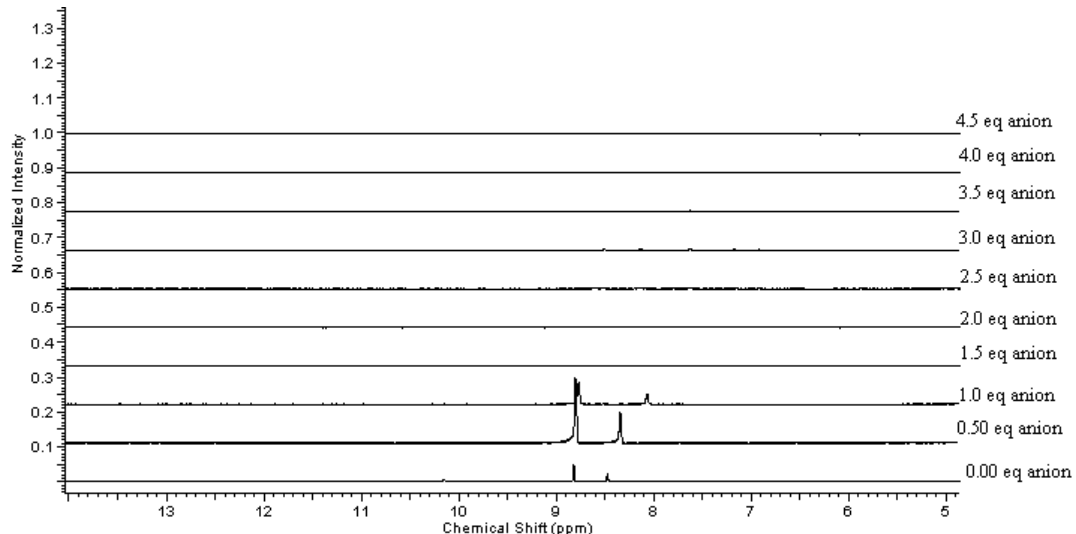


Figure S65: Fit Plot of titration of receptor **3** with TBA hydroxide

6) References

1. S. Perveen, S. M. Abdul Hai, R. A. Khan, K. M. Khan, N. Afza and T. B. Sarfaraz, *Synth. Commun.*, 2005, **35**, 1663.
2. M. Boiocchi, L. Del Boca, D. E. Gomez, L. Fabbrizzi, M. Licchelli and E. Monzani, *J. Am. Chem. Soc.*, 2004, **126**, 16507.
3. M. C. Etter, Z. Urbanczyk-Lipkowska, M. Zia-Ebrahimi and T. W. Panunto, *J. Am. Chem. Soc.*, 1990, **112**, 8415.
4. M. Miyahara, *Chem. Pharm. Bull.*, 1986, **34**, 1950.
5. J. J. Blanksma and G. Verberg, *Recl. Trav. Chim. Pays-Bas*, 1934, **53**, 1037.
6. H. Nowell, S. A. Barnett, K. E. Christensen, S. J. Teat and D. R. Allan, *J. Synchrotron. Radiat.*, 2012, **19**, 435.
7. CrystalClear, Rigaku, 2011.
8. R. Blessing, *J. Appl. Crystallogr.*, 1997, **30**, 421.
9. B. Dittrich, C. B. Hubschle, K. Propper, F. Dietrich, T. Stolper and J. J. Holstein, *Acta Crystallogr., Sect. B.*, 2013, **69**, 91.
10. K. Meindl and J. Henn, *Acta Crystallogr., Sect. A.*, 2008, **64**, 404.
11. M. J. Hynes, *J. Chem. Soc., Dalton Trans.*, 1993, 311.